CONFIDENTIAL

Copy 6
RM E53C17

RM E53C17

NACA

RESEARCH MEMORANDUM

DYNAMIC CHARACTERISTICS OF A SINGLE-SPOOL TURBOJET ENGINE

By R. T. Craig, George Vasu, and R. D. Schmidt

Lewis Flight Propulsion Laboratory
Cleveland, Ohio

NATIONAL ADVISORY COMMITTEE
FOR AERONAUTICS

WASHINGTON

August 7, 1953

CONFIDENTIAL

NACA RM E53C17

NATIONAL ADVISORY COMMITTEE FOR AERONAUTICS

RESEARCH MEMORANDUM

DYNAMIC CHARACTERISTICS OF A SINGLE-SPOOL TURBOJET ENGINE

By R. T. Craig, George Vasu, and R. D. Schmidt

SUMMARY

Operation of a single-spool turbojet engine with variable exhaust-nozzle area was investigated over a range of altitudes at a constant flight Mach number. Data were obtained by subjecting the engine to approximate step disturbances in the independent variables, and the information necessary to effect a linearized first-order description of the engines dynamic operation was obtained.

The generalized dynamic characteristics were little affected by operation at different altitudes but did vary with rotational speed and exhaust-nozzle area. The engine time constant was not noticeably affected by the size and the direction of the fuel flow disturbance used in its determination, but the rise ratios of the other dependent variables were. The data indicated that these step-size effects may be attributed largely to combustion-efficiency changes during off-equilibrium operation. The use of the linearized first-order description of the engine was found to give acceptable accuracy for only very small independent variable disturbances.

INTRODUCTION

Analysis of turbojet-engine control systems can be simplified through the use of analytical techniques in which part or all of the physical system is replaced with its mathematical equivalent. A particularly attractive feature of this technique is that many characteristics of a complete control system can be determined and studied without the necessity of operating the engine under actual or simulated flight conditions. The design of an integrated control system for a turbojet engine requires, however, a knowledge of the dynamic characteristics of the engine.

The mode of engine operation under examination largely will determine the type of analytical approach used. If only stability and response to small perturbations are considered, a linearized first-order description of the engine in matrix form can be very useful (refs. 1 to 3). Determination of the effects of afterburner operation on the primary controlled engine is an example in which this mathematical description can be used advantageously.

In initiating an experimental control program on a new or unexplored turbojet engine, it is possible, on the basis of previous experience with related types, to draw a general picture of the characteristics of the engine to be studied. The status of information available on turbojet-engine dynamics at the start of the investigation covered herein may be summarized as follows:

Engine time-constant values essentially are independent of whether they are determined by the use of fuel flow or exhaust-area step disturbances. Generalized values of time constants, gains, and rise ratios vary with changes in engine rotational speed but are invariant with changes in flight altitude. Effects of size of step disturbances on time constants have not been noticed in a limited number of studies, and no effort has been made in exploring the same effects on rise ratios (ref. 4). Operation at different exhaust-nozzle areas does not affect time constant, and area effects on gains and rise ratios have not been fully explored.

The information presented in this report will substantiate many of these concepts and refute others. Particular attention will be directed to the areas that have received little previous investigation.

The objectives of the work reported herein are to delineate the regions of applicability of the linear representation of the turbojet engine and to discuss some of the difficulties that may be encountered in its use. In addition, the investigation illustrates the degree to which various parameters will generalize for changes in flight condition, the extent to which the dynamic characteristics such as time constants and rise ratios are affected by variations in the size and direction of an input disturbance, and the amount that the dynamic terms used in the description of the engine will vary with changes in exhaust-nozzle area.

A single-spool turbojet engine was installed in the altitude wind tunnel at the NACA Lewis laboratory and investigated at a Mach number of 0.17 at altitudes of 15,000, 35,000, and 45,000 feet. From the experimental program, information sufficient to permit a linear description of the engines dynamic behavior over a range of flight conditions was obtained.

ENGINE DYNAMICS

Previous investigations (refs. 1, 3, and 4) have demonstrated that for stability and small-disturbance studies a set of linearized first-order differential equations may be used to represent the dynamic behavior of a turbojet engine. Therefore, the rotational-speed response of the engine to variations in fuel flow and exhaust-nozzle area may be expressed by the following equations:

$$\Delta N = \left.\frac{\partial N}{\partial W}\right|_A \Delta W + \left.\frac{\partial N}{\partial A}\right|_W \Delta A + \frac{1}{\left.\frac{\partial Q}{\partial N}\right|_{W,A}} \Delta Q \tag{1}$$

$$\Delta N = \frac{1}{\tau_s}\left(-\frac{\Delta Q}{\left.\frac{\partial Q}{\partial N}\right|_{W,A}}\right) \tag{2}$$

(The symbols used are defined in appendix A.) If a general output or dependent variable X is considered, its response to fuel flow and exhaust-nozzle-area perturbations may be expressed by the following:

$$\Delta X = \left.\frac{\partial X}{\partial W}\right|_A \Delta W + \left.\frac{\partial X}{\partial A}\right|_W \Delta A - \left.\frac{\partial X}{\partial N}\right|_{W,A}\left(-\frac{\partial Q}{\left.\frac{\partial Q}{\partial N}\right|_{W,A}}\right) \tag{3}$$

Compressor-discharge pressure, turbine-discharge pressure, net thrust, and turbine-discharge temperature may be expressed in the general form of equation (3).

A convenient arrangement of these equations in matrix form is shown in figure 1, and the mathematical analysis is discussed in detail in references 2 and 3. Each horizontal row of the matrix gives a solution for a particular dependent variable. The solution is understood to be the input to each column multiplied by the coefficient in that column with the summation carried out across each row. The terms shown in the first two columns of the matrix are partial derivatives evaluated with respect to one independent variable while all others are held constant. These terms may be obtained as the slopes of steady-state curves. The partial derivative terms in the third column of the matrix give the time variation of the particular parameter, are evaluated with all independent variables held constant, and must be obtained by use of transient data.

The time variation of rotational speed can be characterized by a first-order time lag; therefore, the use of a time constant is permitted. The time constant is proportional to the polar moment of inertia of the rotating members and is inversely proportional to the rate of change with speed of the difference in torque generated by the turbine and that absorbed by the turbine and that absorbed by the compressor. It is defined as $\tau = -\frac{I}{\left.\frac{\partial Q}{\partial N}\right|_{W,A}}$. The time constant also may be considered to be the time required for 63 percent of any given change in speed to occur in response to a step disturbance in an independent variable.

If so desired, equations (1) to (3) may be manipulated into transfer function form. The response of speed and the general dependent variable X in transfer function form are given by the following equations:

$$\Delta N = \left.\frac{\partial N}{\partial W}\right|_A \frac{1}{(1+\tau s)} \Delta W + \left.\frac{\partial N}{\partial A}\right|_W \frac{1}{(1+\tau s)} \Delta A \tag{4}$$

$$\Delta X = \left.\frac{\partial X}{\partial W}\right|_A \frac{1+a\tau s}{1+\tau s} \Delta W + \left.\frac{\partial X}{\partial A}\right|_W \frac{1+b\tau s}{1+\tau s} \Delta A \tag{5}$$

The values a and b are rise ratios and are a ratio of the initial rise to the final change in a dependent variable caused by either a fuel flow or an area disturbance (ref. 4). The two sets of equations ((1) and (3); (4) and (5)) are related by the following expressions which give the rise ratios in terms of partial derivatives:

$$a = 1 - \frac{\left.\frac{\partial N}{\partial W}\right|_A \left.\frac{\partial X}{\partial N}\right|_{W,A}}{\left.\frac{\partial X}{\partial W}\right|_A} \tag{6}$$

$$b = 1 - \frac{\left.\frac{\partial N}{\partial A}\right|_W \left.\frac{\partial X}{\partial N}\right|_{W,A}}{\left.\frac{\partial X}{\partial A}\right|_W} \tag{7}$$

In these equations the rise ratios a and b and the partial derivative $\left.\frac{\partial X}{\partial N}\right|_{W,A}$ are the terms that are evaluated from transient data. Since the derivative $\left.\frac{\partial X}{\partial N}\right|_{W,A}$ is common to both equations, it is evident that, once the rise ratio for either an area or a fuel flow input is determined, the other rise ratio can be calculated without the need for further transient data. A pitfall in this calculation, however, is that the desired result is contained in a small difference between two numbers of the same approximate size. Therefore, any errors made in the experimental determination of the derivatives or rise ratios become greatly amplified when the results are obtained.

APPARATUS AND PROCEDURE

The information presented in this report was obtained from a turbojet engine having a single-spool axial-flow compressor, an annular combustor, and a variable-area clam-shell-type exhaust nozzle. At static sea-level rated conditions, the compressor pressure ratio was approximately 5 and the rotational speed was 7260 rpm. For the experimental program, the engine was wing mounted in the test section of the NACA Lewis laboratory altitude wind tunnel.

The engine was installed with a bellmouth inlet in order to obtain equivalent flight speeds by use of the tunnel drive system rather than by an inlet ram pipe. Utilization of the tunnel drive system has the advantage that essentially constant flight speed can be maintained during transient operation. However, at the time of the experimental program, difficulties with the drive system limited the maximum flight Mach number to 0.17.

The basic type of disturbance used was an approximate step change in fuel flow. In order to obtain such disturbances, the fuel valve and the pumping system furnished with the engine were replaced by a fuel pump driven by an electric motor and a fuel valve specially designed to obtain short response times and good steady-state stability over a wide range of fuel flows.

A limited number of exhaust-nozzle-area disturbances also were included in the experimental procedure. These disturbances were obtained by introducing a step change in the signal to the electronic-hydraulic nozzle actuator.

For each transient run, the engine was allowed to reach a desired equilibrium flight condition and then was subjected to a step disturbance in either fuel flow or exhaust area. Following this disturbance the engine would accelerate to and level out at a new equilibrium condition. The transients were run in groups of steps from a given condition, up to a new equilibrium value, and then back down to the starting condition. These groups were repeated at a particular value of altitude and exhaust-nozzle area until the complete speed range was covered and then were repeated a sufficient number of times so that all the desired combinations of altitude and exhaust-nozzle area were explored. A similar process was carried out for the area steps with fuel flow held constant in this instance.

Engine parameters were recorded during transients on two, six-channel, direct-inking oscillographs. An example of a typical engine response to a fuel flow disturbance is shown in figure 2. Only the traces under consideration in this report are shown. Table I summarizes

the instrumentation used to measure values in steady state, the sensing device used to measure the variations during transients, and the frequency response of the transient instrumentation. A description of the transient instrumentation is given in appendix B.

ANALYSIS OF EXPERIMENTAL DATA

As indicated in the section ENGINE DYNAMICS, the terms in the first two columns of the matrix of figure 1 can be evaluated as the slopes of steady-state plots. For example, if the gain of speed to fuel flow is considered, a set of curves of speed and fuel flow for the desired flight condition is obtained and the slope of a constant-area line is determined at particular values of speed and fuel flow. In order to determine how well altitude performance can be predicted by use of sea-level data, the steady-state characteristics from each flight condition are generalized to a static sea-level reference. Examination of the slopes of these generalized curves will show whether or not generalization holds. If the data does generalize, then one set of curves can be used for the prediction of many flight conditions.

If the input disturbances are sufficiently close to steps and the instrumentation effects are negligible, the time constant and the rise ratios may be read directly from the experimental results; however, this is seldom possible. In order to overcome these difficulties, the use of semilog plots of the dependent variables against time has proven to be an economical procedure. These semilog plots also eliminate errors introduced by the curvilinear coordinates of the original data, average out random reading errors, and help to overcome any low signal-noise ratios encountered. In addition, since only ratios of values from each trace are used, effects of calibration errors are eliminated. For any particular transient, the various dependent variables can be plotted as a group of parallel straight lines whose slope contains the information necessary to evaluate the engine time constant. Departures from these straight lines provide a measure of the systems deviation from a true first-order linear response.

Determination of the partial derivatives $\left.\frac{\partial X}{\partial N}\right|_{W,A}$ in the third column of figure 1 requires a somewhat more complex treatment than does the time constant. These derivatives can be evaluated directly by taking slopes of the dependent variables during transient operation. This method, however, while very straight forward, does not have a useful degree of accuracy. The poor accuracy can be attributed to reading errors in obtaining the slopes of noisy traces, inherent errors in determining the slopes of traces recorded on a curvilinear coordinate system, and difficulties in calibrating individual traces.

Many of these sources of error can be eliminated or minimized if the transient data are evaluated in the form of rise ratios. It is reasonable, therefore, that the approach to the determination of the derivatives $\left.\frac{\partial X}{\partial N}\right|_{W,A}$ which proved successful is one involving the use of rise ratios. Once the rise ratios and the necessary gain terms are available, the desired partial derivatives can be determined by manipulating equations (6) and (7) into the following expressions:

$$\left.\frac{\partial X}{\partial N}\right|_{W,A} = \frac{\left.\frac{\partial X}{\partial W}\right|_{A} (1 - a)}{\left.\frac{\partial N}{\partial W}\right|_{A}} \tag{8}$$

or

$$\left.\frac{\partial X}{\partial N}\right|_{W,A} = \frac{\left.\frac{\partial X}{\partial A}\right|_{W} (1 - b)}{\left.\frac{\partial N}{\partial A}\right|_{W}} \tag{9}$$

The application of equation (8) or (9) will depend on whether fuel flow or area steps are used for the transient investigation. The gain terms in these equations are from slopes of well-defined steady-state data, and the rise ratios a and b are relatively unaffected by many errors normally found in transient information. Therefore, use of these equations results in one of the most accurate methods available for obtaining values of $\left.\frac{\partial X}{\partial N}\right|_{W,A}$.

RESULTS AND DISCUSSION

All the terms of the matrix of figure 1 will be evaluated, and each dependent variable of the engine will be discussed separately. All data considered will be generalized to static sea-level conditions, and the one-hundred-percent values of all parameters except exhaust-nozzle area are those that would result from operating the engine at rated thrust under sea-level static conditions. The one-hundred-percent value of exhaust-nozzle area is defined as that equal to the turbine-exit area.

Rotational speed. - A steady-state map of the speed - fuel flow performance of the engine is given in figure 3. Data recorded at an altitude of 15,000 feet and a Mach number of 0.17 are generalized to static sea-level conditions. This figure is given only as a typical pattern, because the generalized data taken at other altitudes differ slightly in absolute values. The generalized gains of speed to fuel flow $\left.\frac{\partial N}{\partial W}\right|_A (\delta)$ obtained from curves similar to those of figure 3 are given in figure 4 for three altitudes and four exhaust-nozzle areas. It is evident that the generalized gains for each area are invariant with altitude, but there is a definite effect of exhaust-nozzle area, particularly in the low-speed ranges. In the region above 89 percent rated speed, the gains no longer have a large variation with area and do not change appreciably with speed.

The second column of the matrix is concerned with the area effects on speed. In the interest of simplicity, only one particularly important region of area perturbation, that of maximum speed, will be considered. For each exhaust-nozzle area, a particular fuel flow is required to attain maximum speed and, of course, will vary with flight conditions. In addition, largely because of decreases in combustion efficiency with increased altitude, the generalized fuel flows also will change (fig. 5).

The variation of the gain $\left.\frac{\partial N}{\partial A}\right|_W$ with area and altitude at the maximum speed points is illustrated in figure 6. The data for different areas are evaluated as the slope of a constant fuel flow line at the point of maximum speed with the constant fuel flow being that required to reach maximum speed at the particular exhaust area. The decreasing sensitivity of speed to area changes as operation progresses to the larger areas is clearly shown.

Consideration of the engine time constant now will complete the description of the engine's speed relations. In figure 7 the generalized time constants obtained at various altitudes and by different-size steps in fuel flow and exhaust-nozzle area are presented. These time constants were obtained at various exhaust-nozzle areas. The general shape of the curve is that of a hyperbolic function but with a considerable degree of scatter in the individual data points. As in the case of the speed - fuel flow gains, little variation in time constant with speed was noticed in the range above 89 percent rated speed. An attempt was made to correlate the apparent scatter with altitude, but the degree of scatter at any one altitude was of the same magnitude as that at all altitudes. Efforts to correlate the scatter of time-constant values obtained from fuel steps with exhaust-nozzle area and with the size and direction of the step also failed.

Comparison of the time constants obtained from fuel steps with those from exhaust-nozzle-area steps illustrates that there are no noticeable differences due to the type of disturbance. This result substantiates information from previous studies. Plus and minus speed changes up to the order of 10 percent of rated values were utilized during the program, and over this range no departures from linearity and no effects of step size were discerned in the speed information.

2806

Compressor-discharge pressure. - The steady-state variation of compressor-discharge pressure with fuel flow is shown in figure 8. The form of these data is typical of all altitudes considered. The gains $\left.\frac{\partial P_2}{\partial W}\right|_A$ shown in figure 9 follow the same general trends as the speed - fuel flow gains. The generalized gains are invariant with altitude, show the largest variation with exhaust-nozzle area in the low-speed range, and show little variation with speed in the high-speed regions.

No deviation from the speed - exhaust-nozzle-area pattern is observed in the gains $\left.\frac{\partial P_2}{\partial A}\right|_W$. These generalized values vary with altitude for the smaller areas and then essentially become invariant with altitude in the large areas (fig. 10). As operation progresses to the larger areas, area variations have less effect on the engine.

In figure 11(a) the compressor-discharge-pressure rise ratio d for varied-size steps in fuel flow and for several altitudes is plotted against generalized speed. The data points cover a range of exhaust-nozzle areas. These data points show a considerable degree of scatter and at first inspection do not necessarily justify the single curve drawn. Correlation of the apparent scatter with altitude and exhaust-nozzle area was explored, but none could be ascertained. Such performance paralleled the characteristics exhibited by the engine time constant.

A further attempt to resolve the apparent scatter was made by considering the effects of the fuel flow step size, and the results of this investigation are shown in figure 11(b). For this plot of compressor-discharge-pressure rise ratio for fuel flow steps, the data points of figure 11(a) were used with the points separated into groups of plus and minus 2 percent about a center speed value. With the 100-percent center speed group used for an example, the data points for that particular group were obtained from final speeds of 98 to 102 percent rated and were plotted against the size of total speed change experienced by each transient. The points in any speed group are for a number of altitudes and for a number of exhaust-nozzle areas. In all the ranges considered, there is an essentially straight-line relation of rise ratio to size of speed change. The larger a step up to a final speed, the smaller the

rise ratio; and the larger a step down, the larger the rise ratio. Such behavior holds throughout the speed range, becoming more pronounced at the maximum speed end, and is evidence of definite nonlinear performance.

For infinitesimally small step disturbance, the rise ratio is defined by the intersection of the generalized speed lines of figure 11(b) with a vertical line drawn through the zero-speed-change point ($\Delta N/\sqrt{\theta} = 0$). Transfer of these intersection points to figure 11(a) defines the single curve that is drawn. This curve represents the rise-ratio variation with speed and holds only for very small disturbances; because of the excellent correlation of the apparent scatter with step size, it now appears to be well defined.

After the rise-ratio curve is defined and the speed and compressor-discharge-pressure fuel flow gains are obtained, the partial derivative $\left.\frac{\partial P_2}{\partial N}\right|_{W,A}$ may be calculated by use of equation (6). Generalized values of $\left.\frac{\partial P_2}{\partial N}\right|_{W,A}$ against speed for four exhaust-nozzle areas are given in figure 12. The calculation of these values depends for good results on accurately determining small differences between large numbers. Any errors made in the larger numbers will appear in magnified form in the desired answers; however, cross checks on the generalized values of $\left.\frac{\partial P_2}{\partial N}\right|_{W,A}$ in figure 12 seem to indicate the calculation procedure has a degree of accuracy sufficient to produce useful results. One check is to examine the generalized $\left.\frac{\partial P_2}{\partial N}\right|_{W,A}$ information obtained by taking point-by-point slopes of the transient traces. The data obtained by this method do not define the same curves as in figure 12, but do substantiate the general characteristics of the results obtained by the calculation procedure.

A more precise method by which to check on the calculation of $\left.\frac{\partial P_2}{\partial N}\right|_{W,A}$, and in doing so check the general accuracy of the various gain terms as well, is to substitute the value of $\left.\frac{\partial P_2}{\partial N}\right|_{W,A}$ in equation (7) in order to calculate the rise ratios for area steps. Theoretically, because of the choked condition of the turbine nozzles, the compressor-discharge-pressure rise ratio for an area step should be zero in the high-speed range, and the limited number of area steps taken exhibit this expected behavior. Therefore, if the calculated values of compressor-discharge-pressure rise ratio for area steps are zero for the top-speed

range, the experimental information can be deemed sufficiently accurate. A table of the ratios calculated for exhaust-nozzle-area steps at maximum speed for four areas and two altitudes is tabulated as follows:

Exhaust nozzle area, percent rated area	133	108	98	89
Rise ratios, altitude of 15,000 ft	0.03	0.03	0.07	0
Rise ratios, altitude of 35,000 ft	0.01	-0.06	-0.03	-0.08

All these rise ratios are sufficiently close to zero to support the validity of the use of the experimental data in the calculation procedure.

The difference in the effects of step size on the rise ratio of compressor-discharge pressure and engine time constant brings forth an important point. Previous investigations (ref. 1) have shown that the stability of a controlled engine speed - fuel flow loop adequately can be predicted by use of a linear first-order representation of the engine. Because the time constant of the engine under consideration in this report did not vary noticeably with step size, its speed relation also can be predicted. If other control loops are considered, compressor-discharge pressure with fuel flow, for example, the value of rise ratio in calculations is open to question. The curve of zero-step-size rise ratios in figure 11(a) can be utilized for approximate calculations of response and stability; but once disturbances other than very small ones are considered, cognizance must be taken in the calculation procedure of the rise-ratio variation. This procedure deviates from the simple linear representation and must be used for disturbances in which the speed departs from equilibrium by more than two or three percent. The first two columns of the matrix would still be applicable, but the speed or time effects of column three would not. It also is possible that the time constant of speed-time traces have step-size effects that are not discernible by use of semilog plot analysis. Such action appears probable in that the parameters having the lead-lag form such as compressor-discharge pressure inherently are more sensitive to initial variations in step data than are parameters, such as speed, having the lag form.

Turbine-discharge pressure. - The performance of the steady-state turbine-discharge pressure with fuel flow is shown in figure 13. From similar curves, the gains $\left.\frac{\partial P_6}{\partial W}\right|_{W,A}$ of figure 14 are obtained. Here it is seen that the generalized gains are invariant with altitude, and in

[redacted]

addition they show little variation with exhaust-nozzle area. The three areas other than the largest have essentially the same gains, and all the area curves show little variation over the entire speed range.

The generalized gain $\left.\frac{\partial P_6}{\partial A}\right|_W \left(\frac{1}{\delta}\right)$ in figure 15 exhibits the same characteristics as those exhibited by speed and compressor-discharge pressure. The gains vary with altitude and become essentially constant in the larger areas. The variation with altitude is more noticeable in this case, however, than in the case of compressor-discharge pressure.

2806

The rise ratios of turbine-discharge pressure for fuel flow steps are shown in figure 16. The plot of rise ratio against speed change in figure 16(b) illustrates that the step-size effects are considerably less than those experienced for compressor-discharge pressure. If the change in speed necessary to cause a certain percent variation in the rise ratios of compressor-discharge pressure is considered, a considerably larger change in speed is necessary to cause the same percent variation in the rise ratios of turbine-discharge pressure. An additional cause of separation can be noted here, however. In the speed range above 87 percent rated, effects of the exhaust-nozzle area become significant. In figure 16(b) the two nozzles that are 133 and 108 percent of the rated area are represented by the dot-dash lines, and the two nozzles that are 98 and 89 percent of the rated area are shown by the dashed lines. Below 87 percent rated engine speed, all areas are represented by the solid curves. These data show that, for any given speed above 87 percent rated, the rise ratio at the small areas is noticeably lower than at the large areas. Both still exhibit the step-size characteristic. The two curves in figure 16(a) are the zero-step-size intercepts of the lines of figure 16(b). A single curve is drawn in the region below 87 percent rated speed. The separation may be in four groups rather than two, but there was insufficient data to define any such action. The two areas in each group have a common characteristic. The two larger areas are larger than the turbine-exit area, while one of the two smaller areas is essentially equal to the turbine-exit area and the other is smaller. This action suggests that the place or manner in which the engine chokes is tied in with the rise ratios obtained downstream of the choked region.

From the two curves of rise ratio, the partial derivative terms $\left.\frac{\partial P_6}{\partial N}\right|_{W,A}$ may be determined, and they are shown in figure 17. The general characteristics exhibited by compressor-discharge pressure are followed by the turbine-discharge pressure.

Net thrust. - Previous studies had indicated that the behavior of net thrust and turbine-discharge pressure would be very similar, and this was in part substantiated herein.

The performance map of steady-state scale thrust against fuel flow is shown in figure 18. These values differ from net thrust by the drag of the experimental installation, which was not determined. The data for the exhaust nozzle of 133 percent rated area cannot be shown on the same coordinates because these data were run with an installation having slightly different drag characteristics.

In figure 19 it can be seen that the generalized gains of thrust to fuel flow $\left.\frac{\partial F}{\partial W}\right|_A \sqrt{\theta}$ are very similar to those of turbine-discharge pressure in their variation with speed, exhaust-nozzle area, and altitude. For constant-area curves, no variations with altitude are detected; and the three smaller areas of 89, 98, and 108 percent rated area have essentially the same values of gains. The area of 133 percent rated area has somewhat smaller gains throughout the speed range, and all curves show that thrust is increasingly less sensitive to area changes in the large areas.

The thrust experimental information was somewhat limited, and thrust - exhaust-nozzle-area gains at top speed were obtained only at two areas. Values of this gain $\left.\frac{\partial F}{\partial A}\right|_W \left(\frac{1}{\delta}\right)$ are shown in the following table for a flight Mach number of 0.17 and at rated engine rotational speed:

Altitude, H, ft	Exhaust-nozzle area, A sq in.	
	530	483
	$\left.\frac{\partial F}{\partial A}\right\|_W \left(\frac{1}{\delta}\right)$, $\frac{\text{percent rated thrust}}{\text{percent rated area}}$	
15,000	-0.349	-0.273
35,000	-.355	-.284

As is readily seen, these generalized gains are essentially invariant with changes in altitude and seem to be similar to the patterns set by turbine-discharge pressure.

Further similarity between the results of thrust and turbine-discharge pressure is evidenced in the thrust-rise-ratio results of figure 20. The rise-ratio curve of figure 20(a) is defined by the intersections of the speed group lines in figure 20(b) with a vertical line drawn through the zero-speed-change point. While

the form of this curve is similar to the turbine-discharge-pressure information, several important differences are apparent. There is no separation into two area curves in the high-speed range, and the thrust ratios are approximately 20 to 40 percent lower at rated generalized speed than the turbine-discharge-pressure rise ratios. In addition, figure 20(b) illustrates that the percent variations in thrust rise ratios with size of speed change are larger than the variations shown in the rise ratios of turbine-discharge pressure and are more similar in size to the variations shown by compressor-discharge pressure.

The thrust partial derivative $\left.\frac{\partial F}{\partial N}\right|_{W,A}$ generalized to static sea level is presented in figure 21. These curves are similar to those obtained for compressor- and turbine-discharge pressures with respect to variations with area and generalized speed.

It is of interest that all the partial derivative curves $\left.\frac{\partial X}{\partial N}\right|_{W,A}$ reach maximums in the generalized speed range of 83 to 96 percent rated speed. The trends of peak point with exhaust area are not consistent with area, however.

Turbine-discharge temperature. - The generalized data in figure 22 illustrate the fact that the steady-state characteristics of turbine-discharge temperature against fuel flow are somewhat unique in that increasing the fuel flow does not in all ranges bring about an increase in temperature. Reversals are experienced in the lower fuel flow ranges. Because of these reversals, the temperature - fuel flow gains $\left.\frac{\partial T_6}{\partial W}\right|_A$ experience both positive and negative values as shown in figure 23. Consistent with the other gains considered, the generalized temperature gains are affected by exhaust-nozzle area and speed, but they are invariant with altitude. Only one altitude was explored in the lower-speed range, however; and if data from different altitudes were available in this region, full generalization may not necessarily hold.

In figure 24 the generalized gains of temperature to area $\left.\frac{\partial T_6}{\partial A}\right|_W \left(\frac{1}{\theta}\right)$ are presented. These generalized gains exhibit a consistent variation with the exhaust-nozzle area for the two altitudes investigated, but the two altitude curves are displaced by an increasing amount as operation progresses to the smaller areas.

The information presented on temperature gains exhibits characteristics that essentially follow the patterns set by speed, compressor- and turbine-discharge pressures, and thrust. However, several regions of

severe limitation are encountered when rise ratios are used to determine the value of $\left.\frac{\partial T_6}{\partial N}\right|_{W,A}$, the term descriptive of the time behavior of temperature. Inspection of equation (6) shows that extremely large values of rise ratio, both negative and positive, may be expected at low engine speeds where the steady-state derivative $\left.\frac{\partial T_6}{\partial W}\right|_{A}$ is near zero. In the upper-speed region the rise ratio as experimentally determined is close to unity so that equation (6) again fails to accurately determine $\left.\frac{\partial T_6}{\partial N}\right|_{W,A}$.

Because its rise ratios are such large numbers in the lower-speed region and so close to unity in the higher-speed region, temperature places the largest demands on experimental accuracy of any of the dependent variables considered. However, experimental conditions are such that the temperature data as recorded are affected by the largest amount of unresolvable noise exhibited by any dependent variable. Other parameters such as thrust have lower signal-noise ratios, but the noise is largely caused by vibrations and such effects can be eliminated easily in the analysis of the data.

An attempt was made to circumvent some of the preceding difficulties in determining $\left.\frac{\partial T_6}{\partial N}\right|_{W,A}$ in the following manner: From experimentation of similar engines, consideration of theoretical aspects, and examination of a limited number of area perturbations for the engine under study, it is expected that there is no immediate change in turbine-discharge temperature because of an exhaust-nozzle disturbance, particularly in the high-speed regions. Such action indicates that the rise ratio in turbine-discharge temperature to an area step change is essentially zero in this region. Therefore, it can be seen from the equation for rise ratio

$$j = 1 - \left.\frac{\partial T_6}{\partial N}\right|_{W,A} \frac{\left.\frac{\partial N}{\partial A}\right|_{W}}{\left.\frac{\partial T_6}{\partial A}\right|_{W}}$$

that $\left.\frac{\partial T_6}{\partial N}\right|_{W,A}$ can be determined if the gains $\left.\frac{\partial N}{\partial A}\right|_{W}$ and $\left.\frac{\partial T_6}{\partial A}\right|_{W}$ are known and the rise ratio is assumed zero. Such computed values obtained by utilizing experimentally determined $\left.\frac{\partial N}{\partial A}\right|_{W}$ and $\left.\frac{\partial T_6}{\partial A}\right|_{W}$ gains are shown in figure 25.

Some corroboration of these computed results is available from experimental transient temperature data taken with fuel flow steps. The partial derivative $\left.\frac{\partial T_6}{\partial W}\right|_{A,N}$ was determined from the transient traces, and the generalized data are shown in figure 26. These values show considerably less scatter than any values obtained for rise ratios; but, although the data points show trends for each area, they do not justify the curves drawn. The curves drawn were determined from the following equation: $\left.\frac{\partial T_6}{\partial W}\right|_{A,N} = \left.\frac{\partial T_6}{\partial W}\right|_{A} - \left.\frac{\partial T_6}{\partial N}\right|_{W,A} \left.\frac{\partial N}{\partial W}\right|_{A}$ where $\left.\frac{\partial T_6}{\partial W}\right|_{A}$ and $\left.\frac{\partial N}{\partial W}\right|_{A}$ are determined from steady-state data and $\left.\frac{\partial T_6}{\partial N}\right|_{W,A}$ is taken from figure 25. The calculated curves are within the scatter of the experimental data and have a consistent variation with area that is essentially supported by the individual area points. Since the calculated values agree with the experimental data, the values of $\left.\frac{\partial T_6}{\partial N}\right|_{W,A}$ in figure 25 are considered to be of useful accuracy.

Close examination of the $\left.\frac{\partial T_6}{\partial W}\right|_{A,N}$ values indicates that the size and the direction of the step in fuel flow had a definite effect on the initial rise in temperature, as it did on the other dependent variables considered. Due to the separation into four areas, however, there were insufficient data to eliminate the step-size effects and thus exactly to specify the curves.

Examination of all dependent variables considered indicates that throughout the engine there is a consistent pattern set by the variation of rise ratios with size of fuel flow disturbance. In comparison with an infinitesimally small step, a finite step up to a final speed gives smaller rise ratios and a step down gives larger rise ratios. Such a pattern may be a conventional nonlinearity, which will necessitate expressing the time history of a dependent variable as a function of fuel flow, area, and a time derivative of the dependent variable. In this case the equations used to obtain the matrix form no longer apply, and for very large disturbances a nonlinear analysis undoubtedly is necessary.

Utilization of a nonlinear mathematical treatment may not be necessary, however, if only medium-sized excursions, 10 percent of rated speed or less, are considered. This may be done by assuming that the step-size effects are largely caused by combustion-efficiency variations during off-equilibrium operation. Measured temperature exhibited step-size effects, and it, in general, is a good measure of the true energy input to the engine. In addition, all the dependent variables have a

very consistent variation with step size. These characteristics indicate that the assumption of combustion-efficiency changes during transients is reasonable. If this efficiency does vary with an effective time relation of the same order of magnitude as the engine time constant, the step effects can be accounted for.

Accounting for a combustion-efficiency variation during transient operation would necessitate an addition to the matrix of figure 1. The actual fuel into the engine would be replaced by an effective fuel input. This input would be obtained by operating on the actual fuel flow disturbance by a lead-lag transfer function and then introducing this value into the matrix form. Thus, with a fairly simple addition, the matrix form can be utilized for study of disturbances up to the order of 10-percent changes in rated speed.

SUMMARY OF RESULTS

Operation of a turbojet engine with a variable exhaust-nozzle area was investigated at altitudes of 15,000, 35,000, and 45,000 feet at a constant flight Mach number of 0.17. From the information obtained in these studies, a summary of the dynamic characteristics of the turbojet engine may be made as follows:

1. The generalized fuel flow gains $\left.\frac{\partial X}{\partial W}\right|_A$ of the dependent variables, speed, compressor- and turbine-discharge pressure, net thrust, and turbine-discharge temperature, were invariant with changes in altitude. The generalized gains of exhaust-nozzle area $\left.\frac{\partial X}{\partial A}\right|_W$ of the same dependent variables were found, however, to vary with altitude. The generalized time constants for both the fuel flow and the area steps and the rise ratios for fuel flow steps also were invariant for altitude changes.

2. All fuel and area gains were affected by the value of the exhaust-nozzle area. All area gains reached minimum values in the large areas. No area effects were noted on either time constant or any rise ratios other than those of turbine discharge. The turbine-discharge-pressure rise ratio in the high-speed range varied with exhaust area; the smaller areas gave lower rise ratios. Turbine-discharge-temperature transient information was presented in the form of an initial rise in temperature to a fuel flow step, and these values also were affected by operation at various exhaust-nozzle areas. All partial derivatives of the form $\left.\frac{\partial X}{\partial N}\right|_{W,A}$ were dependent on exhaust-nozzle area.

[redacted]

3. Up to the limit of speed changes investigated, ±10 percent, the engine time constant was independent of the size of step and no departures from linearity were discerned. The rise ratios of compressor-discharge pressure, turbine-discharge pressure, and thrust were affected by the size and direction of the speed change. The data indicated that these step-size effects may be attributed largely to combustion-efficiency changes during off-equilibrium operation. Consideration of the individual parameters gives the degree of rise-ratio variation with size of step to be expected in each case.

4. The use of rise ratios does not appear to be an adequate description of the time behavior of turbine-discharge temperature. Use of the initial rise due to a fuel flow step gave acceptable results; however, the amount of noise encountered made the accuracy of the results more questionable than that of the other dependent variables considered.

Lewis Flight Propulsion Laboratory
National Advisory Committee for Aeronautics
Cleveland, Ohio

[redacted]

APPENDIX A

SYMBOLS

The following symbols are used in this report:

A	exhaust-nozzle area, percent rated area
a,b,d, f,j,k	initial rise ratios
F	net thrust, percent rated thrust
H	altitude, ft
I	rotor polar moment of inertia
N	engine rotational speed, percent rated speed
P_2	compressor-discharge pressure, percent rated pressure
P_6	turbine-discharge pressure, percent rated pressure
Q	engine torque
s	complex Laplacian operator
T_6	turbine-discharge total temperature, percent rated temperature
W	fuel flow, percent rated fuel flow
X	general dependent variable
δ	ratio of total pressure at engine inlet to a reference absolute pressure, at NACA standard sea-level conditions
θ	ratio of total temperature at engine inlet to a reference total temperature, at NACA standard sea-level conditions
τ	engine time constant, sec

[redacted]

APPENDIX B

DESCRIPTION OF TRANSIENT INSTRUMENTATION

Recording equipment. - Engine parameters were recorded during transients on six-channel, direct-inking, magnetic-penmotor oscillographs. Each channel of the recorders was driven by either a d.c. or strain-analyzer type of amplifier, depending on the parameter being measured. Strain-analyzer amplifiers were used with the sensing devices for pressures, fuel flow, and thrust, while d.c. amplifiers were used with the sensing devices for speed, temperature, and position. The frequency response of the penmotors in combination with either type of amplifier is essentially flat over the range from 0 to 100 cycles per second. The oscillograph chart speed was 12.5 millimeters ($2\frac{1}{2}$ units) per second.

Timing marks were introduced on certain channels by removing the signals from these channels, before or after a transient, simultaneously, by means of a switch. These marks serve as a means of alining the traces from different recorders and for detecting slight variations in the length of individual pens.

Position indication. - The position of the exhaust nozzle was obtained by attaching a potentiometer in such a manner that its movable arm was an indication of the position of the nozzle. A d.c. voltage was applied across the potentiometer so that a d.c. voltage indicative of position appeared between the movable arm and either end of the potentiometer. For the transient indication, the initial level of the signal was cancelled out by series addition of an adjustable voltage opposite in polarity to that of the signal. This was done since it was desired to record only the change during the transient. The signal then was applied to a d.c. amplifier feeding one channel of a recorder.

The frequency response of this circuit was limited by that of the amplifier and recorder.

Turbine-discharge temperature. - Turbine-discharge temperature was measured by a number of 18-gage, chromel-alumel, butt-welded thermocouples electrically connected in parallel. The signal from the thermocouples was applied to a magnetic amplifier to increase the amplitude of the signal without the introduction of excessive noise or drift. The magnetic amplifier was followed by an adjustable voltage to cancel out the initial level, a thermocouple compensator, and a d.c. amplifier feeding one channel of a recorder.

The thermocouple compensator is an electric network which, when properly adjusted, compensates for the thermal lag of the thermocouple. A detailed discussion of the basic principles and circuitry involved is

given in reference 5. This device enables a faster response to be obtained with heavy thermocouple wire than could be ordinarily obtained with small wire. Methods for determining the time constant of thermocouples are given in reference 6.

The compensator was set by placing only one thermocouple in the circuit and then suddenly plunging the thermocouple from a cooled shield into the hot gas stream, effectively subjecting the thermocouple to a step change in temperature. The compensator was then adjusted until the temperature trace recorded as nearly a step as possible.

The frequency response of this circuit with the compensator properly adjusted is flat over the range from 0 to 5 cycles per second at sea-level mass-flow conditions.

Engine speed. - An alternator on the engine provides a voltage whose frequency is directly proportional to speed and varies from 300 to 800 cycles per second over the speed range normally encountered. This signal was used in connection with an electronic tachometer which was modified to give an accurate steady-state and suitable transient indication of engine speed.

The steady-state indication is provided by a counting circuit that counts the input frequency for a period of 1.2 seconds, which is accurately set by a crystal-controlled oscillator. This count is then presented on a neon lamp display panel for a suitable length of time, after which the process is repeated. Although the count is very accurate, unless the frequency is high in relation to speed, the speed cannot be precisely defined. Consequently, the alternator signal was first applied to two stages of full-wave rectification which increased the frequency by a factor of four. With this modification, the steady-state speed indication was precise to within 1 rpm.

The transient signal was obtained by modifying an existing meter circuit included in the instrument to provide a continuous indication of frequency and, hence, speed. A d.c. voltage, proportional to speed, is produced by the modified meter circuit. After cancellation of the initial level, this signal was applied to a d.c. amplifier feeding one channel of a recorder.

The frequency response of this circuit is limited by a filter circuit required in the modified meter circuit and is essentially flat over the range from 0 to 10 cycles per second.

Air pressures. - Transient measurements of ram pressure, compressor-discharge pressure, and turbine-discharge pressure were made with the use of standard, four-element, strain-gage pressure pickups and strain-analyzer-type amplifiers. A network in the analyzer provides a means of adjusting the initial output of the amplifier so that only the change need be recorded.

The pressure pickups were mounted in the wing section in a centrally located box which reduced the effect of engine vibration on the pickups.

The dynamic response of these circuits is a function of the diameter and length of the tubing used to transmit the pressure from the engine to the pressure pickup and of the density of the air. Design of tubing size is outlined in reference 7. All tubing was experimentally tested and adjusted before installation to give a frequency response which is essentially flat from 0 to 10 cycles per second at sea-level conditions.

Fuel flow. - The transient indication of fuel flow was obtained by measuring the pressure drop across an orifice in the fuel line by means of a differential strain-gage pressure pickup. The operation of the pressure pickup is the same in this case as for those used to measure air pressures. In order to obtain a sufficiently large pressure drop regardless of the fuel flow, the size of orifice used was made variable by means of a remotely controlled positioning system. The major limitations on the fuel information obtained were the mass and capacitance effects of the fuel and piping system. These limited the useful frequency range to 0 to 2 cycles per second. The pressure measuring device, the fuel valve, and the pressure regulator across the valve produced negligible effects in this frequency band.

Thrust. - The transient thrust measurement, like the pressure measurements, was obtained with a strain-gage and strain-analyzer type of amplifier. In this case, however, the strain gage is bonded to a thrust link attached from the engine to the mount. The engine is supported in such a manner that the total force of the engine is transmitted to the mount through this thrust link.

The frequency response of the circuit to a change in the thrust link is limited by the recorder and amplifier, but the response of the entire system is dependent on the dynamics of the entire mounting system, which has not been determined.

REFERENCES

1. Dandois, Marcel, and Novik, David: Application of Linear Analysis to an Experimental Investigation of a Turbojet Engine with Proportional Speed Control. NACA TN 2642, 1952.

2. Ketchum, J. R., and Craig, R. T.: Simulation of Linearized Dynamics of Gas-Turbine Engines. NACA TN 2826, 1952.

3. Boksenbom, Aaron S., and Hood, Richard: General Algebraic Method Applied to Control Analysis of Complex Engine Types. NACA Rep. 980, 1950. (Supersedes NACA TN 1908.)

4. Delio, Gene J.: Evaluation of Three Methods for Determining Dynamic Characteristics of a Turbojet Engine. NACA TN 2634, 1952.

5. Shepard, Charles E., and Warshawsky, Isidore: Electrical Techniques for Compensation of Thermal Time Lag of Thermocouples and Resistance Thermometer Elements. NACA TN 2703, 1952.

6. Scadron, Marvin D., and Warshawsky, Isidore: Experimental Determination of Time Constants and Nusselt Numbers for Bare-Wire Thermocouples in High-Velocity Air Streams and Analytic Approximation of Conduction and Radiation Errors. NACA TN 2599, 1952.

7. Delio, Gene J., Schwent, Glennon V., and Cesaro, Richard S.: Transient Behavior of Lumped-Constant Systems for Sensing Gas Pressures. NACA TN 1988, 1949.

[redacted]

TABLE I. - INSTRUMENTATION

Measured quantity	Steady-state instrumentation	Transient instrumentation	
		Sensor	Range over which frequency response is essentially flat, cps
Fuel flow	Rotameter	Aneroid-type pressure sensor, with strain-gage element, connected to measure pressure drop across a variable orifice in fuel line	Undetermined
Exhaust-nozzle area	Potentiometer attached to rack and gear assembly and connected in electric circuit to give indication on microammeter; microammeter reading converted to area	Control feedback potentiometer	0-100
Ram pressure	Water manometers	Aneroid-type pressure sensor, with strain-gage element	0-10 at sea-level static
Compressor-discharge total pressure	Mercury manometers	Aneroid-type pressure sensor, with strain-gage element	0-10 at sea-level static
Turbine-discharge total pressure	Alkazene manometers	Aneroid-type pressure sensor, with strain-gage element	0-10 at sea-level static
Thrust	Scale	Strain gage mounted on strain link attached to forward engine suspension	0-100
Turbine-discharge total temperature	Twenty-four individual thermocouples connected to potentiometer-type strip-chart record	Six, paralleled, 18-gage, chromel-alumel, butt-welded thermocouples and electric network to compensate for thermocouple lag	0-5 at sea-level static when used with properly adjusted compensator

$$(1)\quad \Delta N = \left.\frac{\partial N}{\partial W}\right|_A \Delta W + \left.\frac{\partial N}{\partial A}\right|_W \Delta A + \frac{1}{\left.\frac{\partial Q}{\partial N}\right|_{W,A}} \Delta Q$$

$$(2)\quad \Delta N = \frac{1}{\tau s}\left(-\frac{\Delta Q}{\left.\frac{\partial Q}{\partial N}\right|_{W,A}}\right)$$

$$(3)\quad \Delta X = \left.\frac{\partial X}{\partial W}\right|_A \Delta W + \left.\frac{\partial X}{\partial A}\right|_W \Delta A - \left.\frac{\partial X}{\partial N}\right|_{W,A}\left(-\frac{\Delta Q}{\left.\frac{\partial Q}{\partial N}\right|_{W,A}}\right)$$

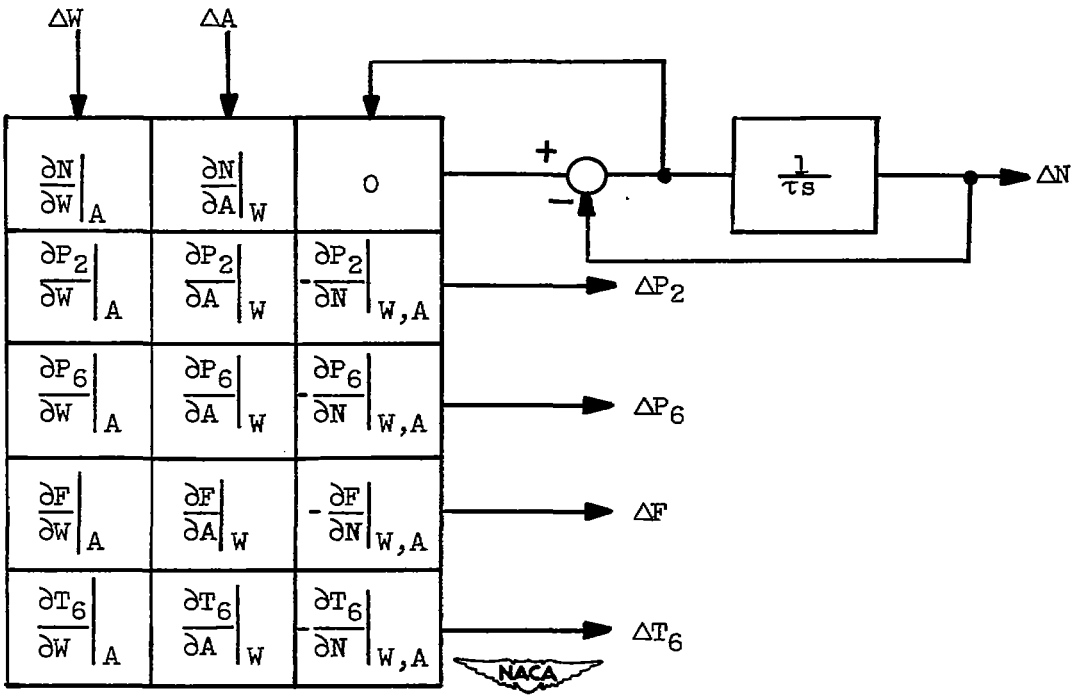

Figure 1. - Matrix form used in linearized description of dynamic characteristics of turbojet engine.

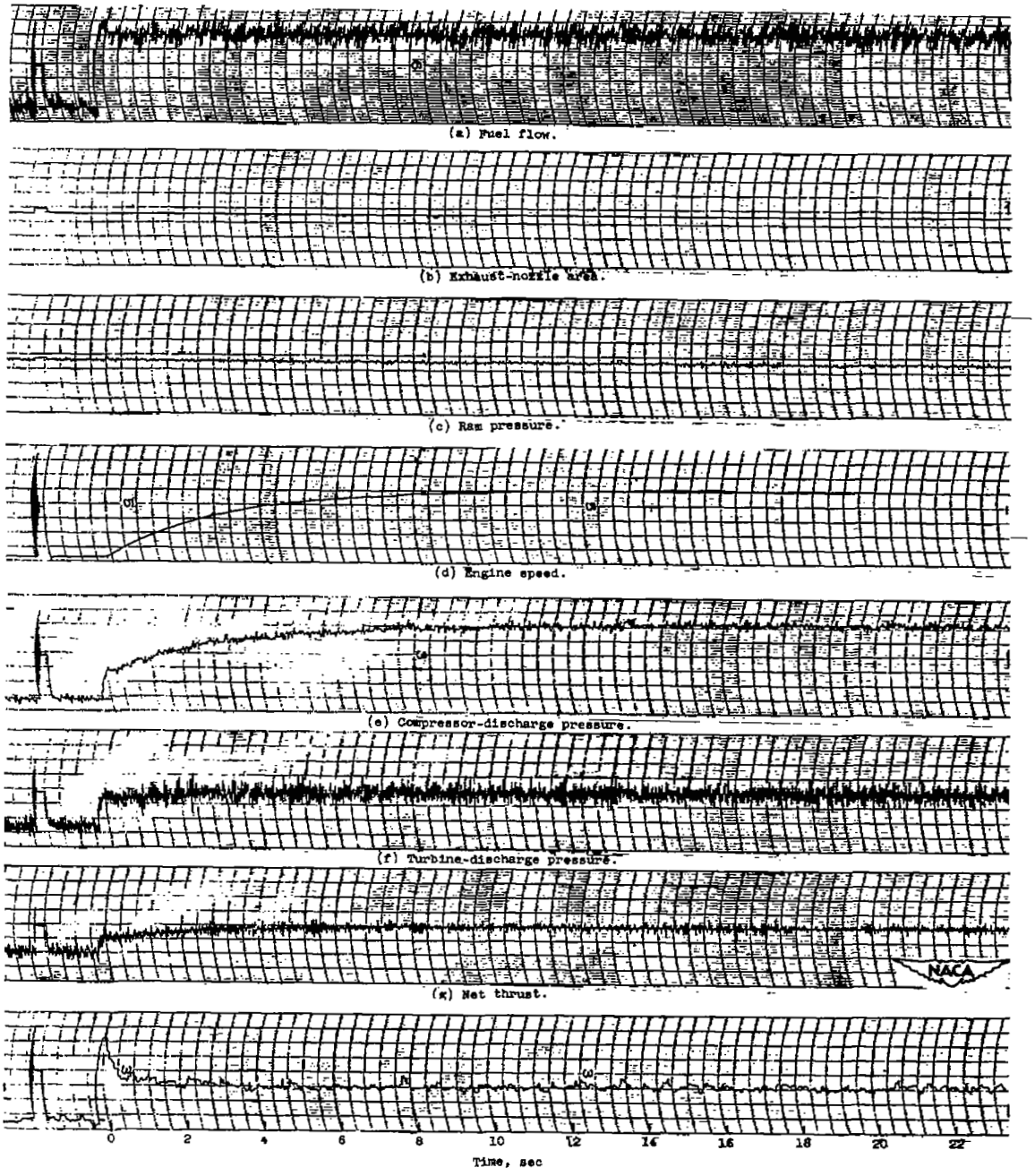

Figure 2. - Oscillogram of response of turbojet engine to an approximate step change in fuel flow. Altitude, 15,000 feet; Mach number, 0.17.

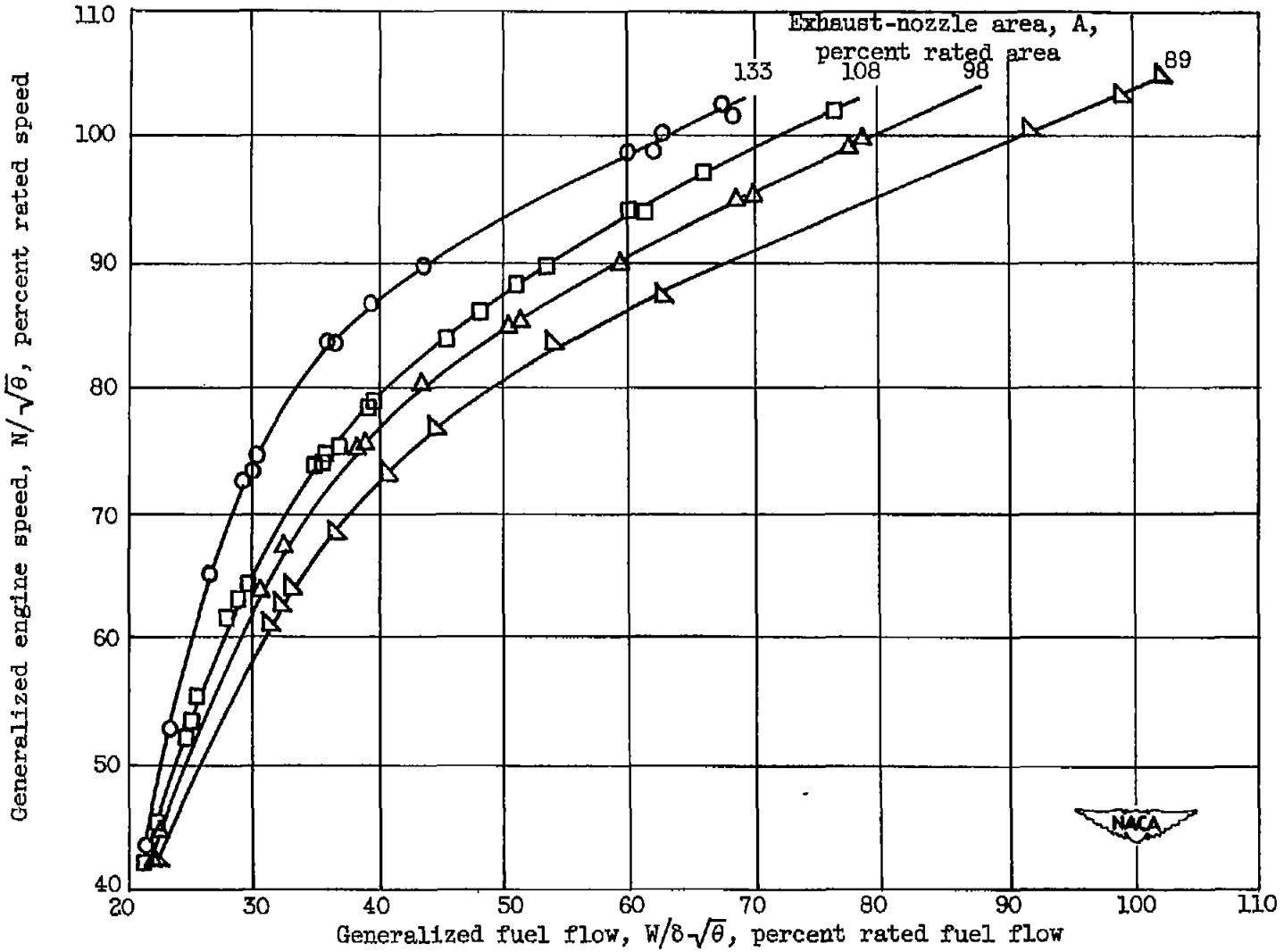

Figure 3. - Variation of generalized engine speed with fuel flow. Altitude, 15,000 feet; Mach number, 0.17.

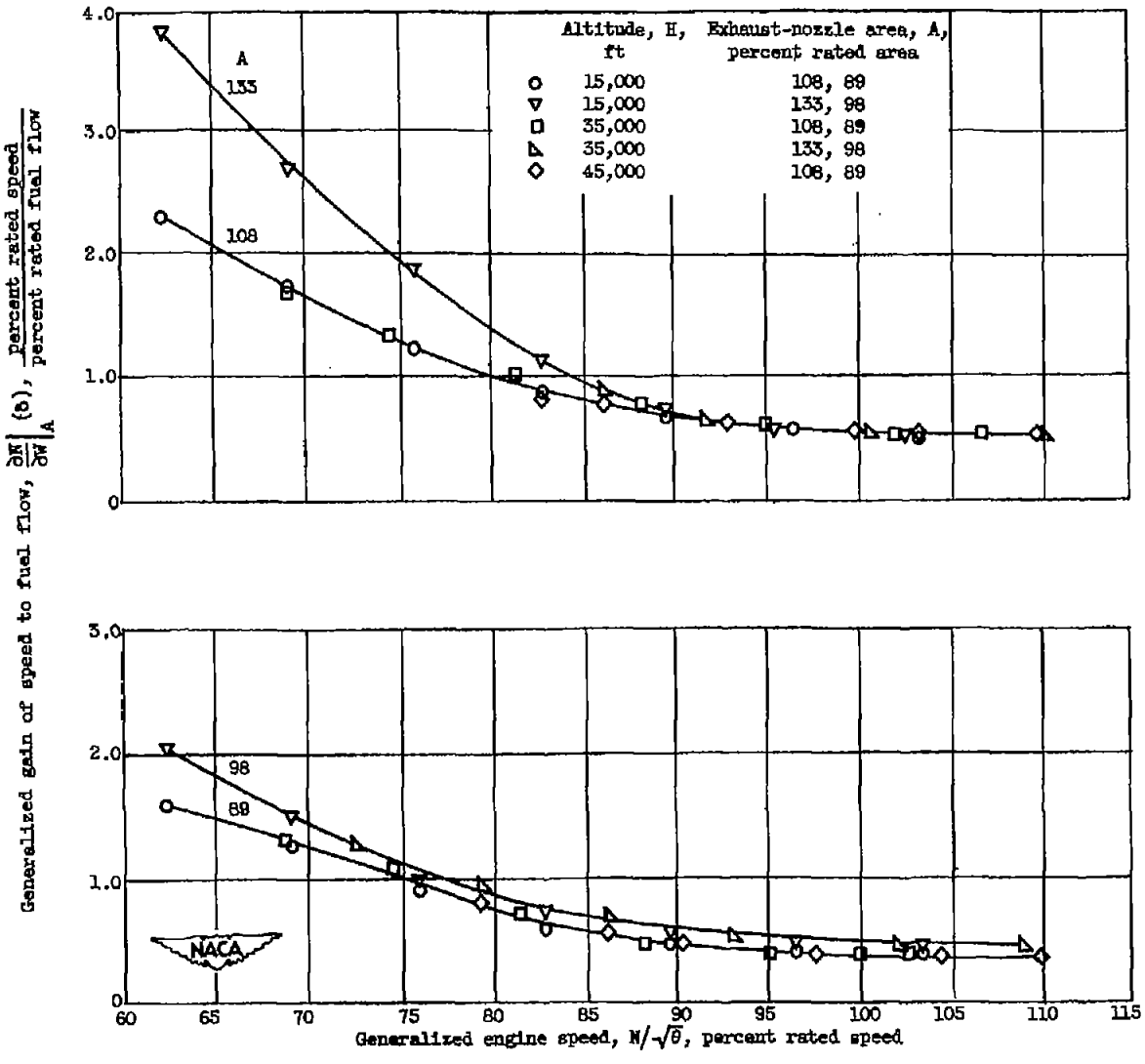

Figure 4. - Variation of generalized gain of speed to fuel flow with engine speed.

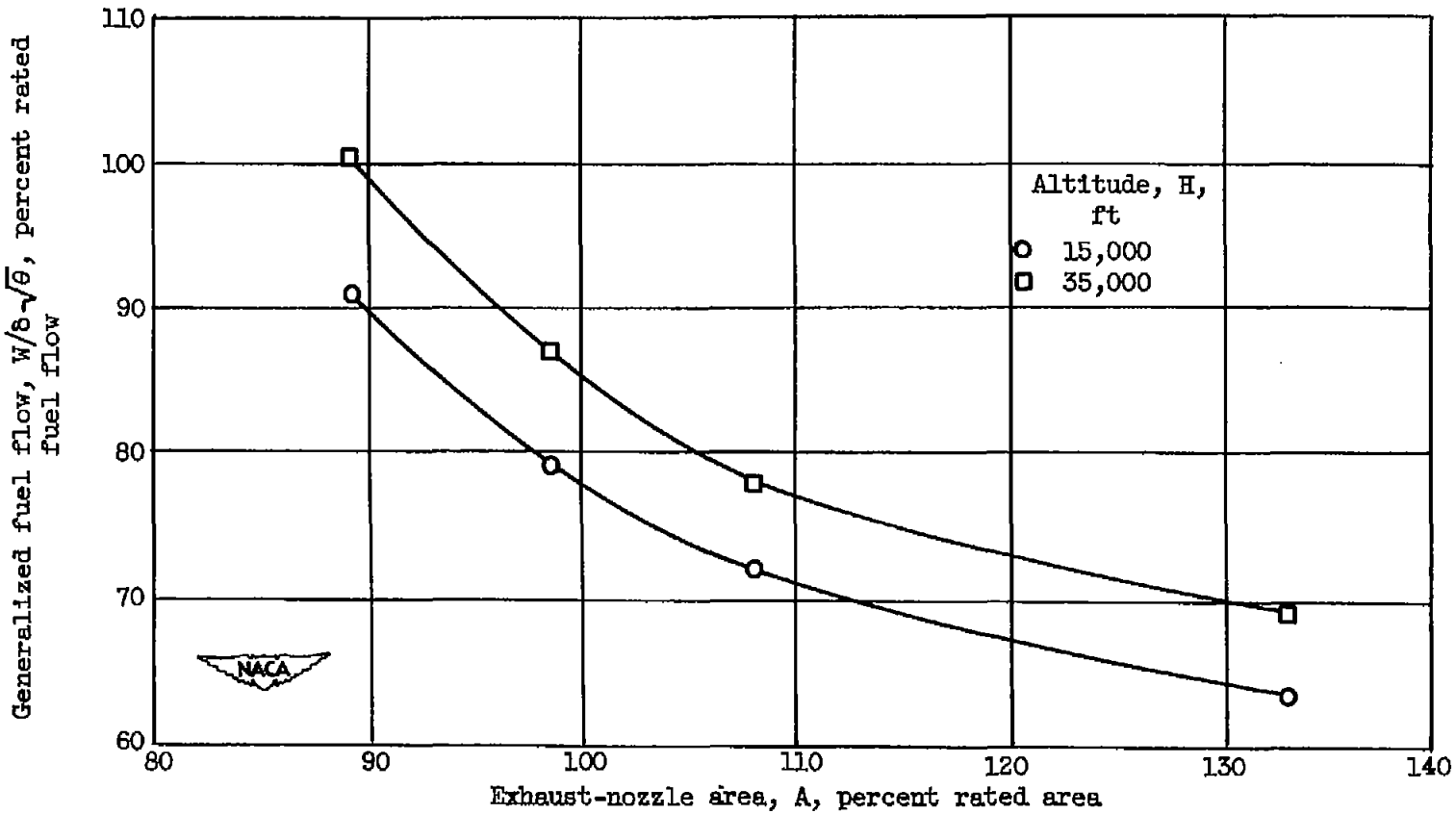

Figure 5. - Variation of generalized fuel flow with exhaust-nozzle area at 100 percent rated engine speed.

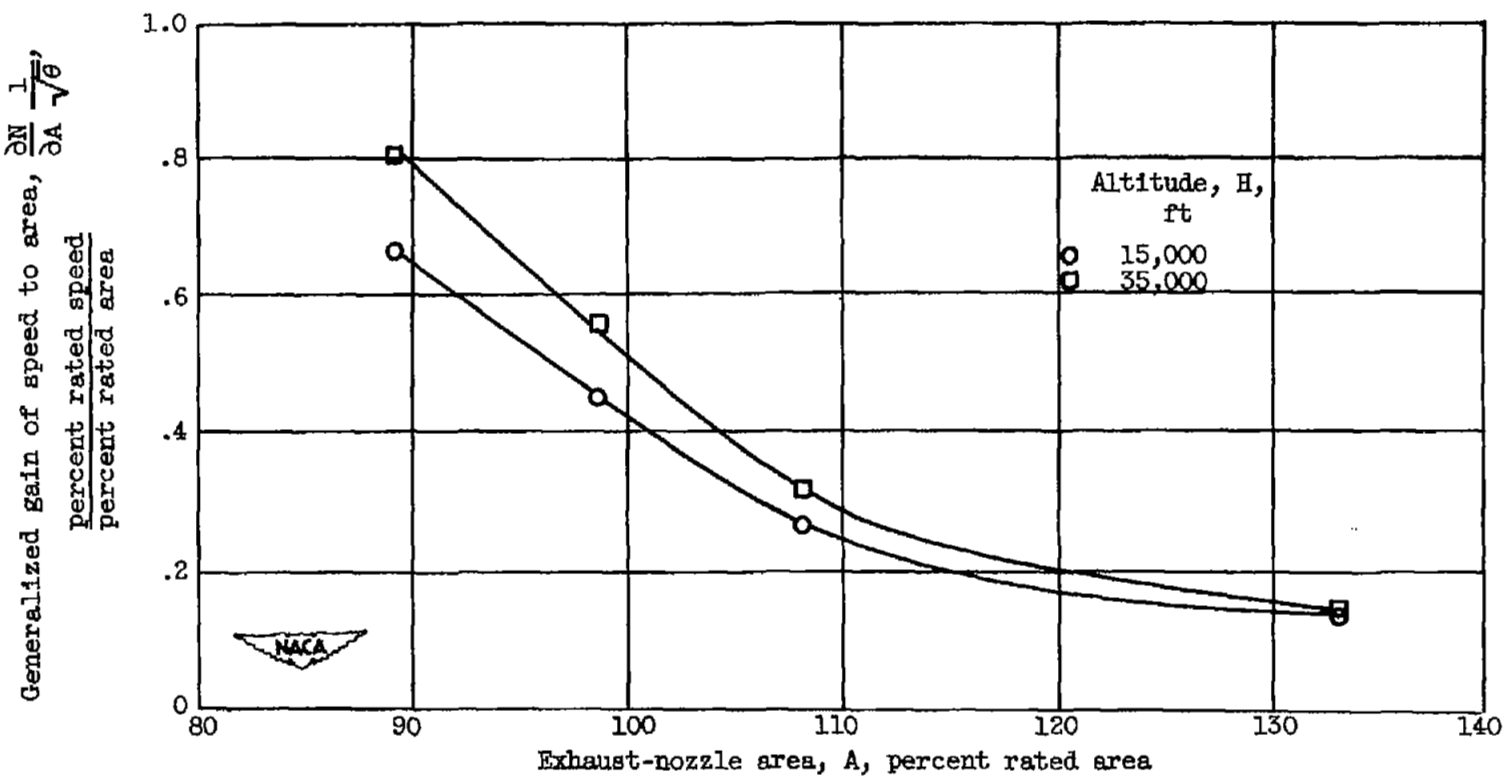

Figure 6. - Variation of generalized gain of speed to area with exhaust-nozzle area at 100 percent rated engine speed.

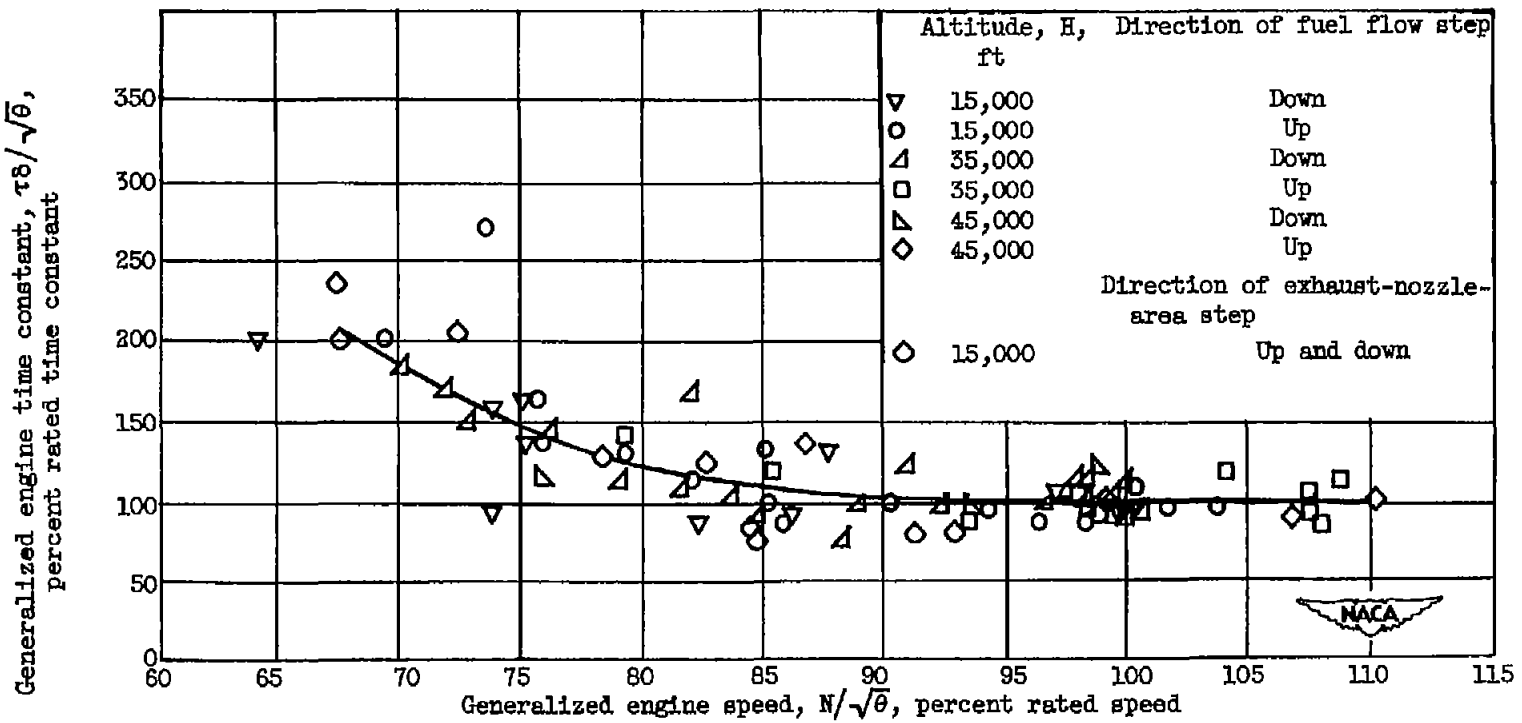

Figure 7. - Variation of generalized engine time constant with engine speed.

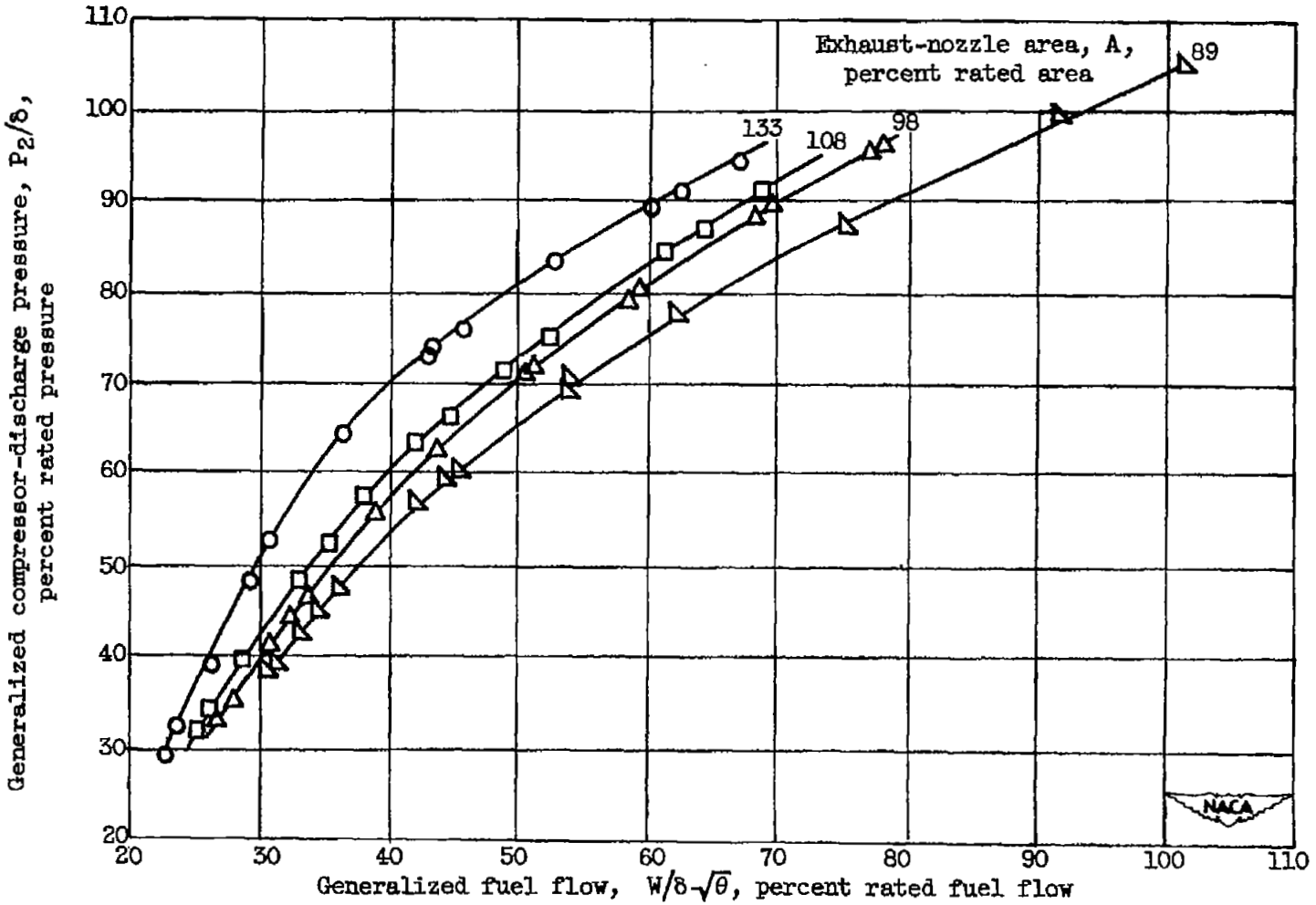

Figure 8. - Variation of generalized compressor-discharge pressure with fuel flow. Altitude, 15,000 feet; Mach number, 0.17.

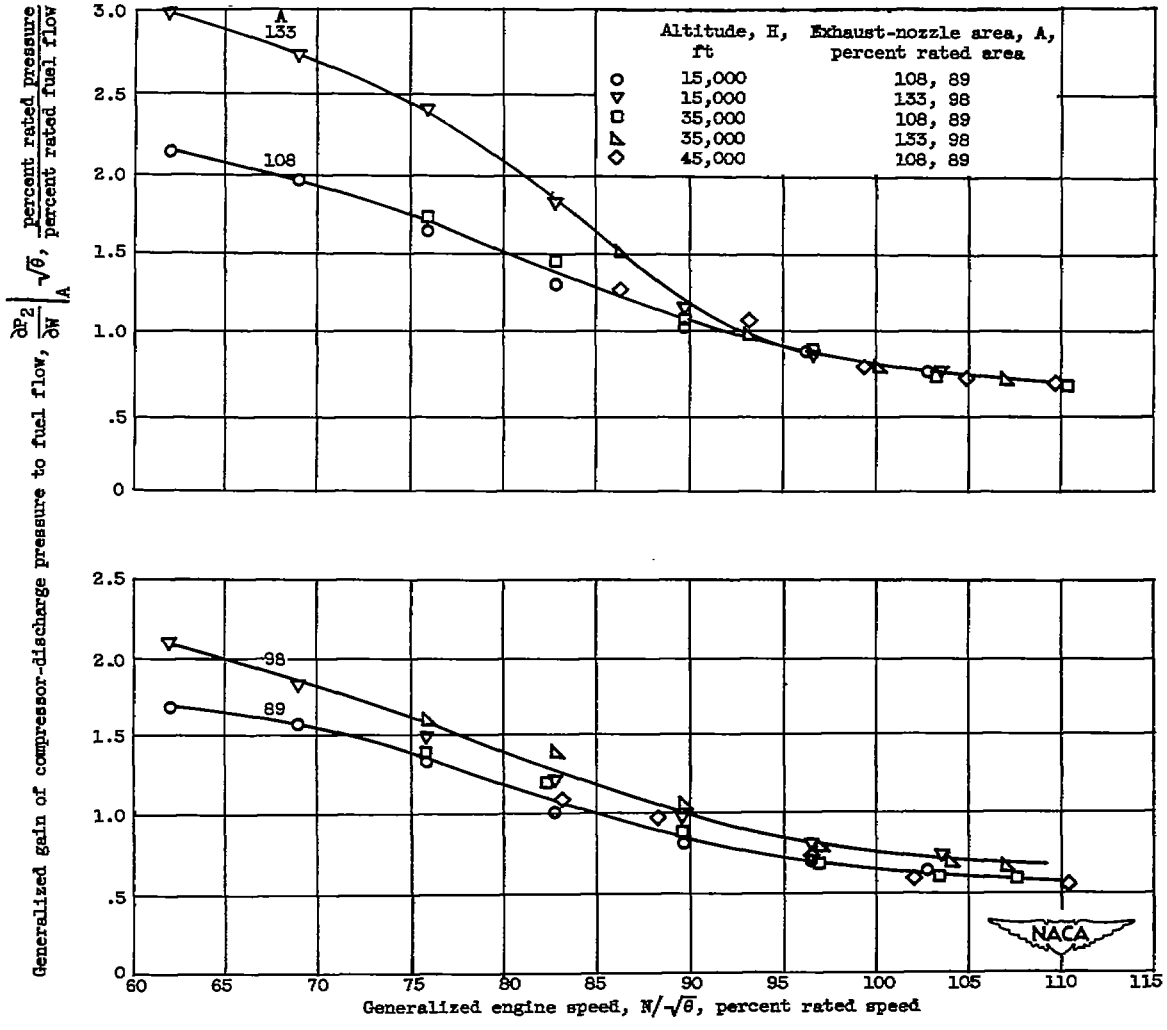

Figure 9. - Variation of generalized gain of compressor-discharge pressure to fuel flow with engine speed.

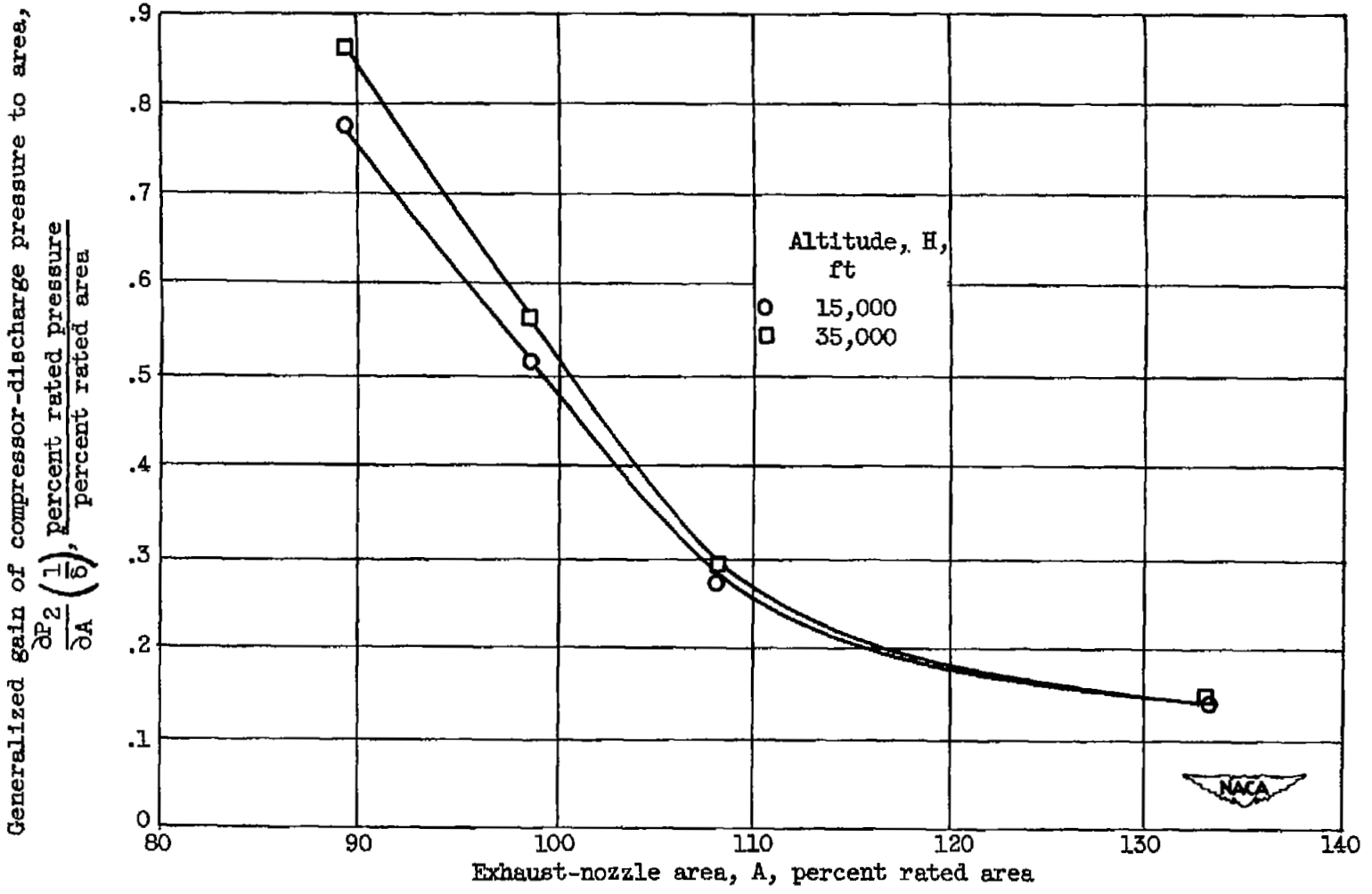

Figure 10. - Variation at 100 percent rated engine speed of generalized gain of compressor-discharge pressure to area with exhaust-nozzle area.

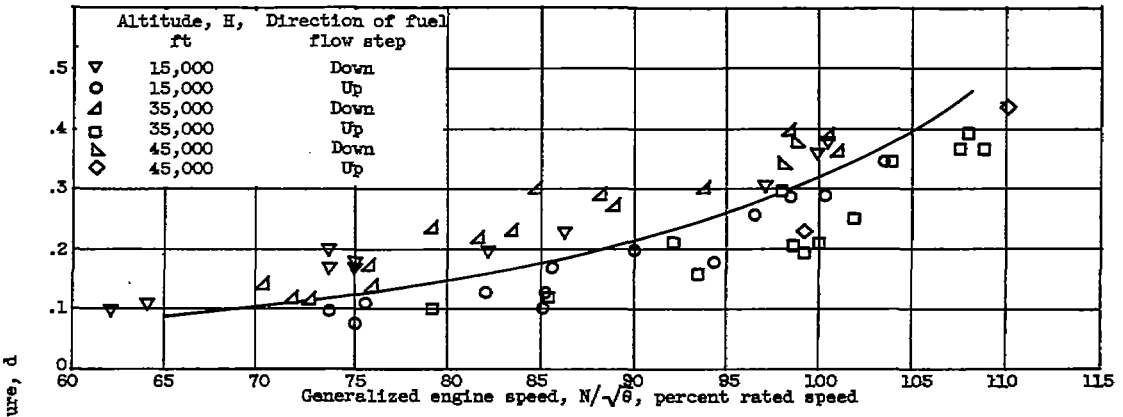

(a) Generalized engine speed.

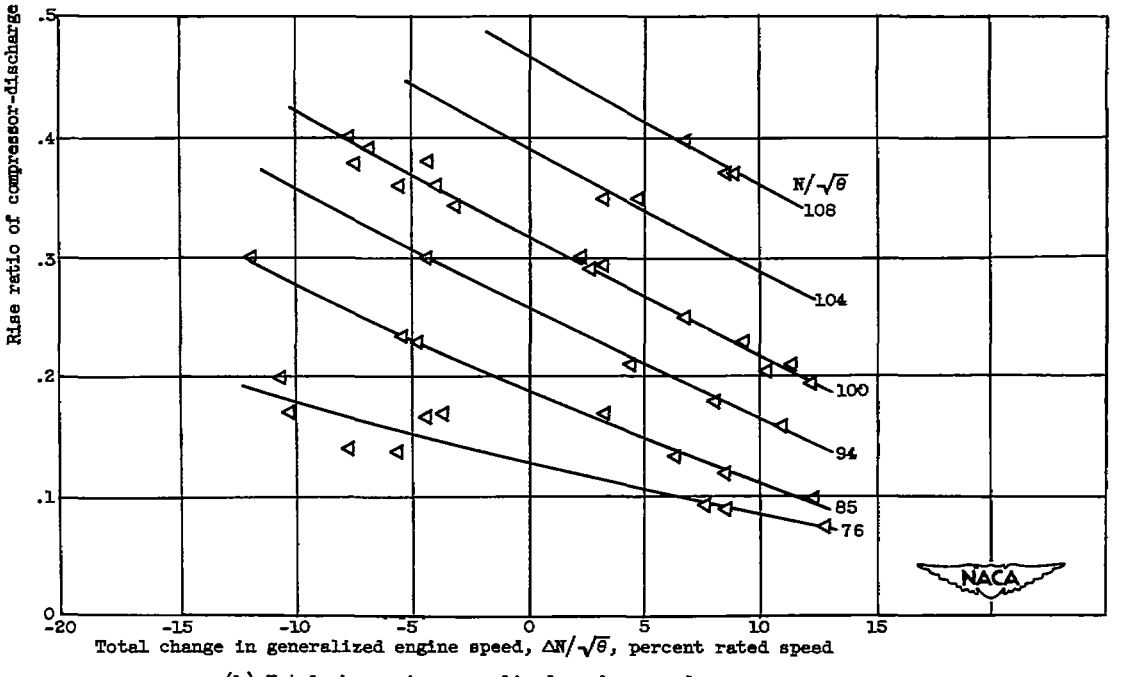

(b) Total change in generalized engine speed.

Figure 11. - Variation of rise ratio of compressor-discharge pressure with generalized engine speed and with engine speed change.

[redacted]

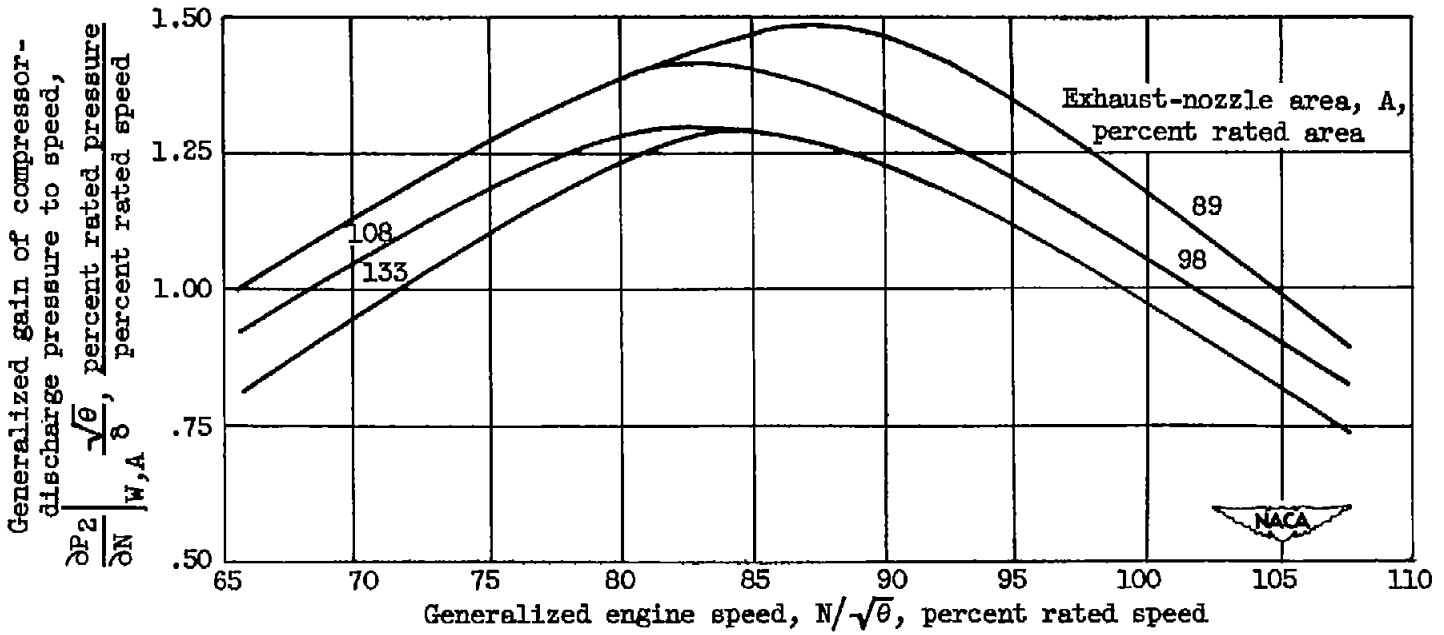

Figure 12. - Variation of generalized gain of compressor-discharge pressure to speed with engine speed.

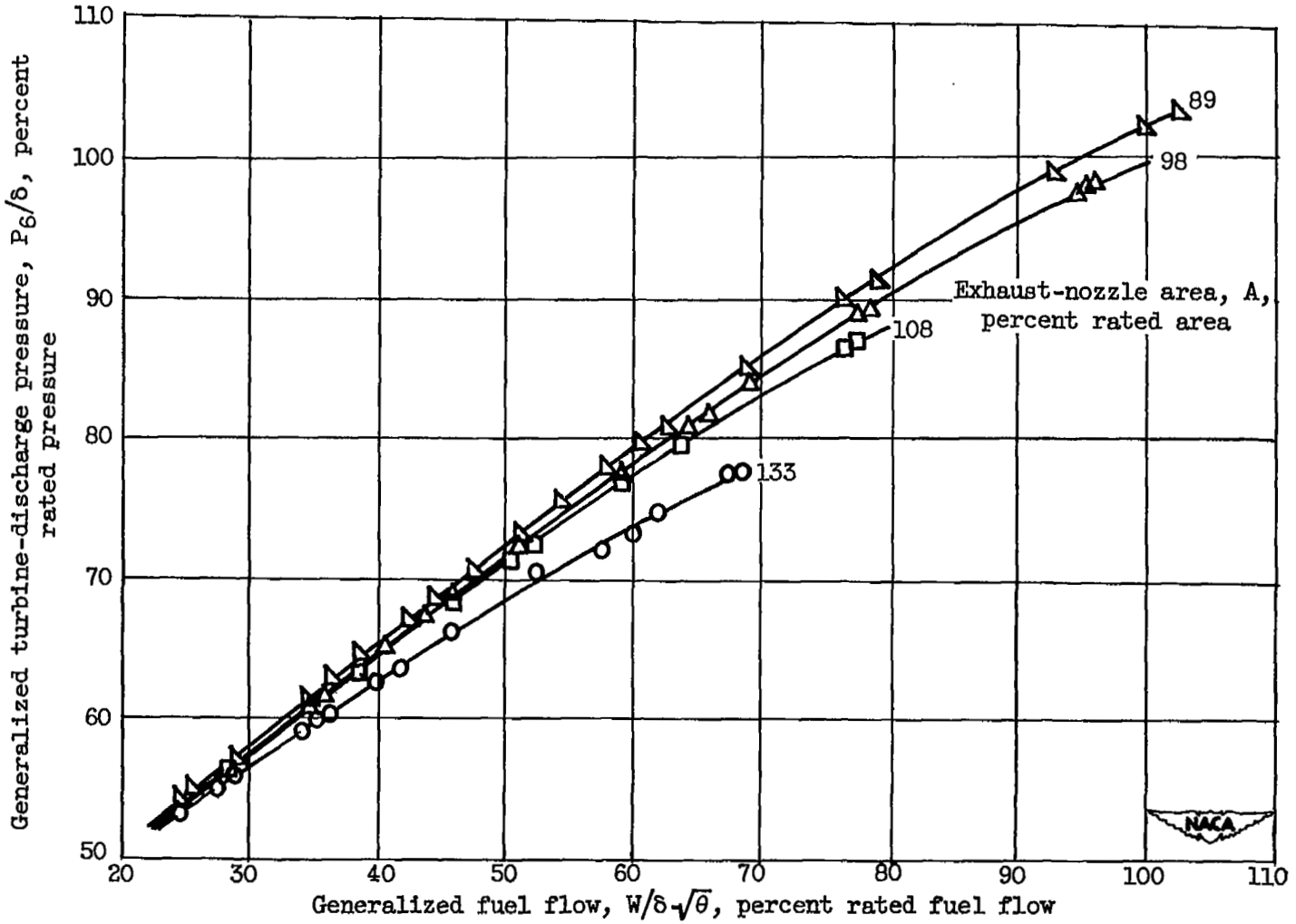

Figure 13. - Variation of generalized turbine-discharge pressure with fuel flow.

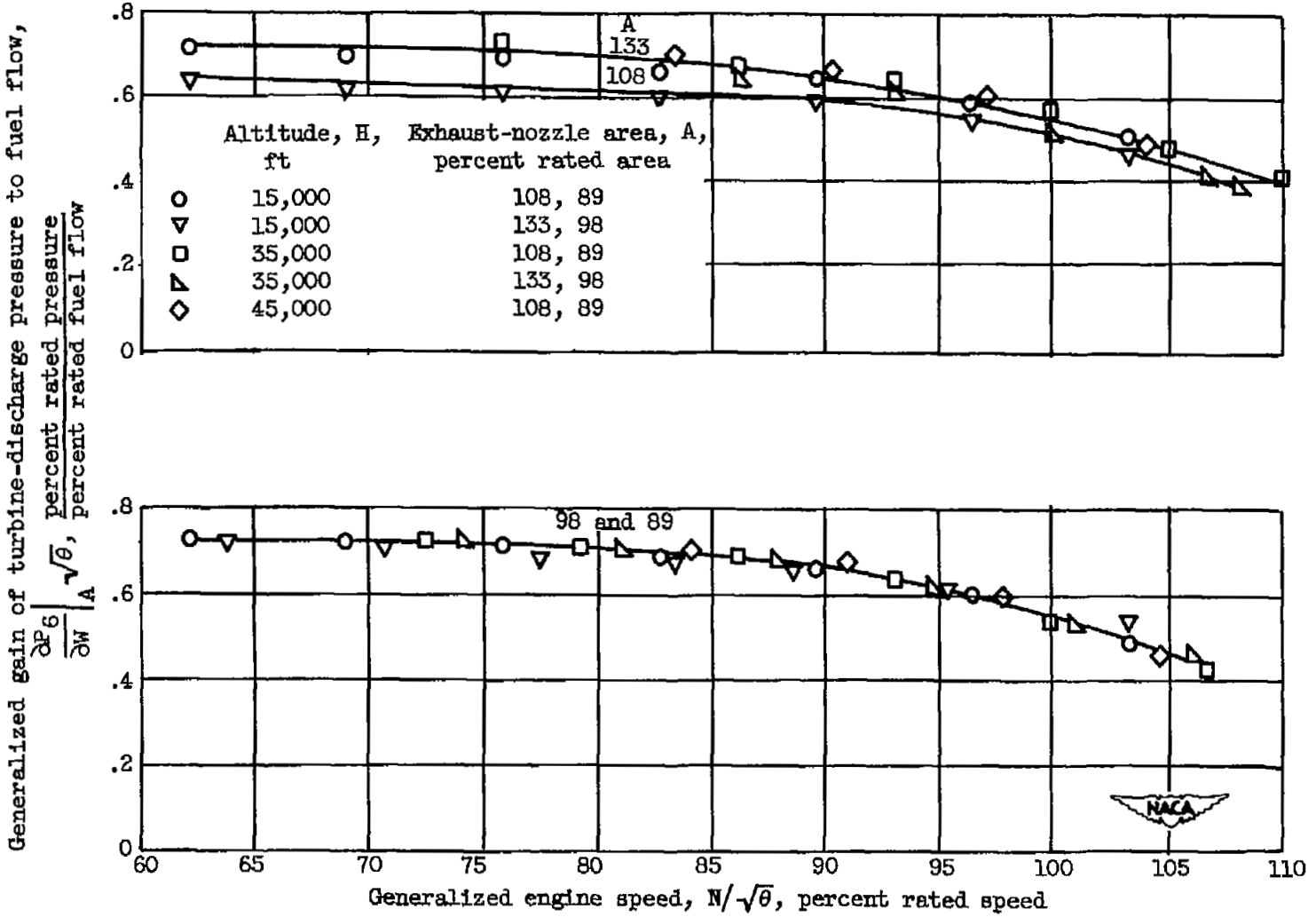

Figure 14. - Variation of generalized gain of turbine-discharge pressure to fuel flow with engine speed.

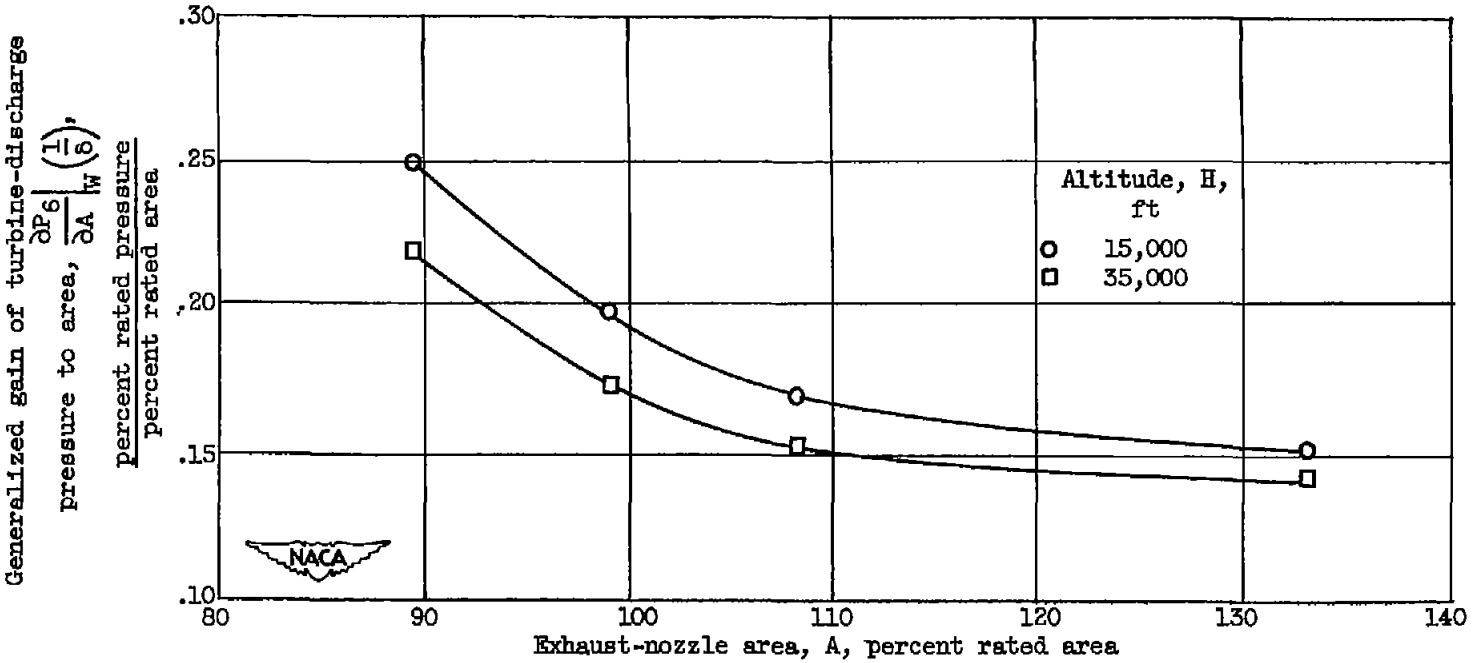

Figure 15. - Variation at 100 percent rated engine speed of generalized gain of turbine-discharge pressure to area with exhaust-nozzle area.

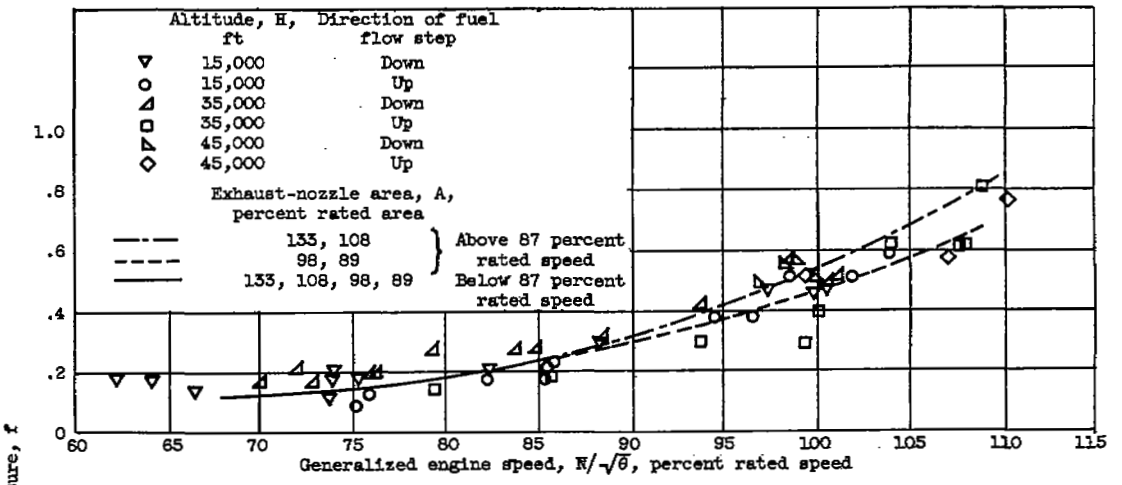

(a) Generalized engine speed.

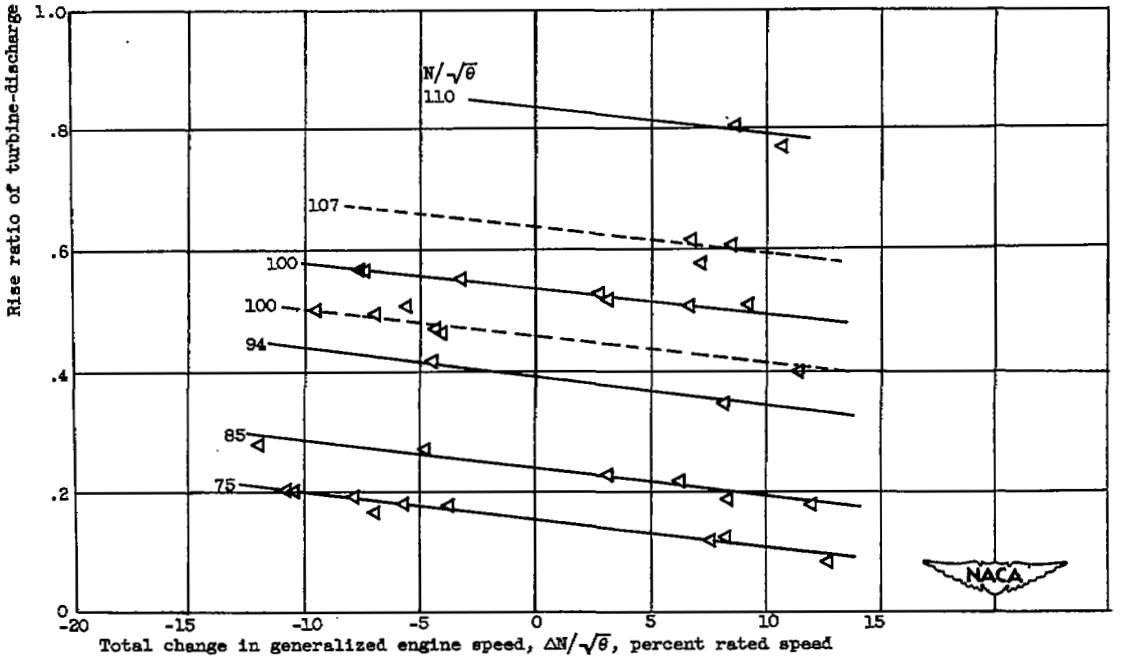

(b) Total change in generalized engine speed.

Figure 16. - Variation of rise ratio of turbine-discharge pressure with generalized engine speed and engine speed change.

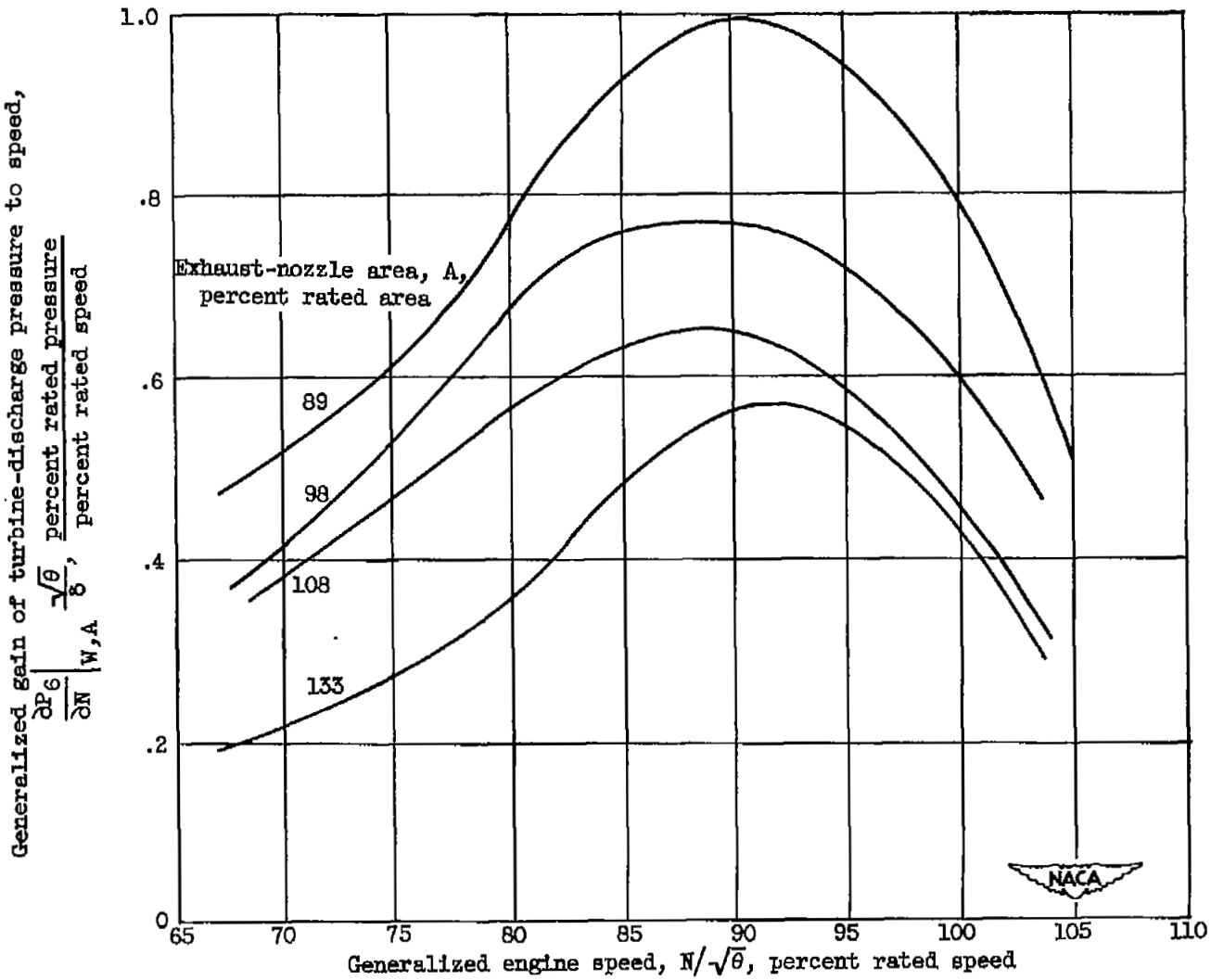

Figure 17. - Variation of generalized gain of turbine-discharge pressure to speed with engine speed.

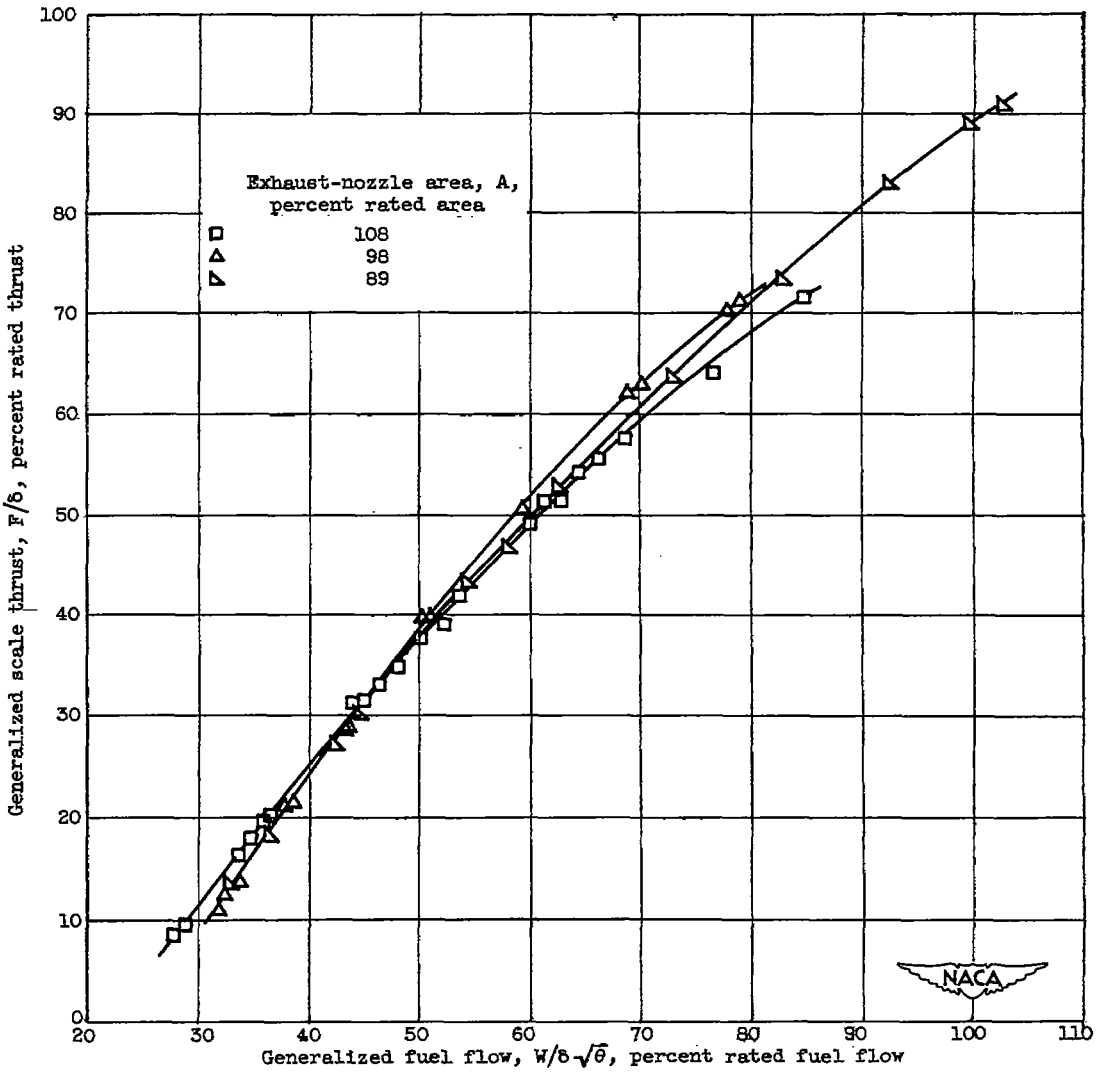

Figure 18. - Variation of generalized scale thrust with fuel flow. Altitude, 15,000 feet; Mach number, 0.17.

[redacted]

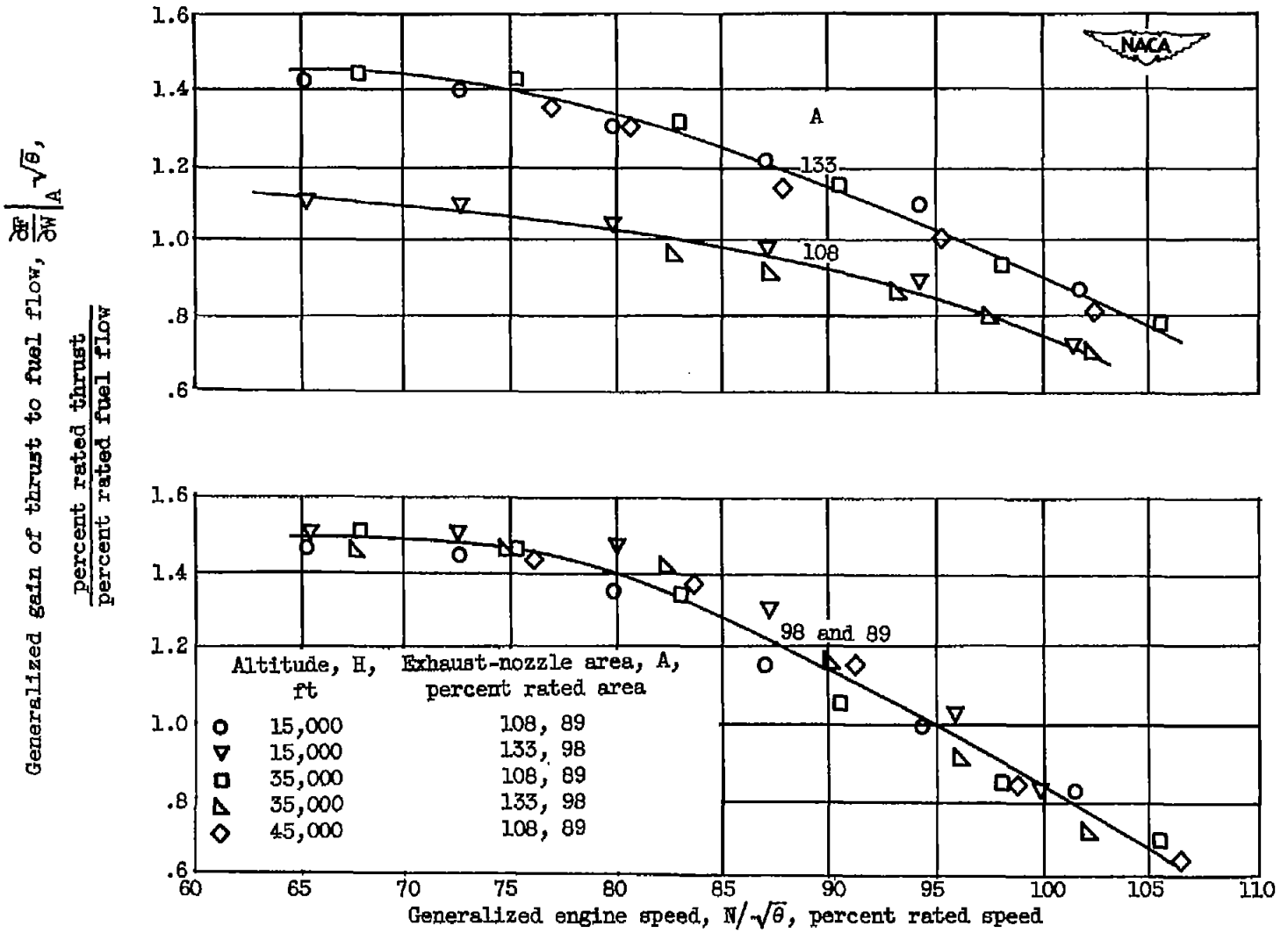

Figure 19. - Variation of generalized gain of thrust to fuel flow with engine speed.

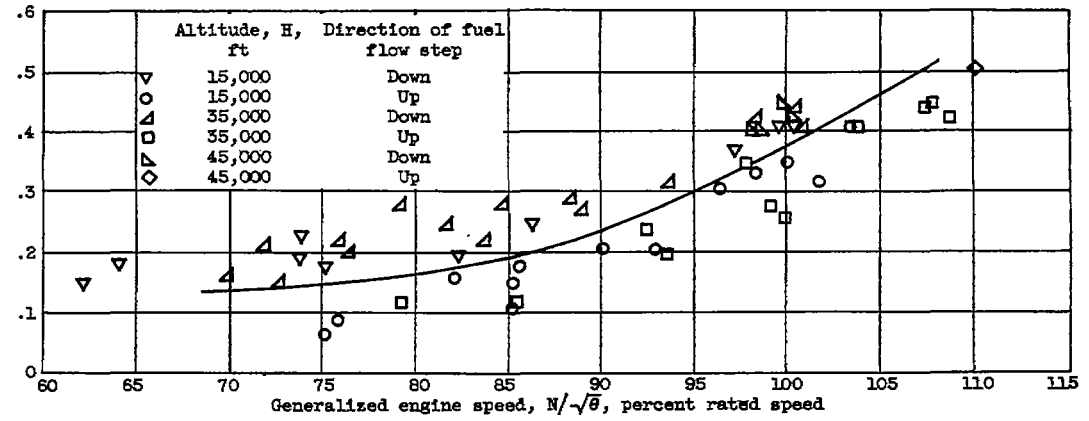

(a) Generalized engine speed.

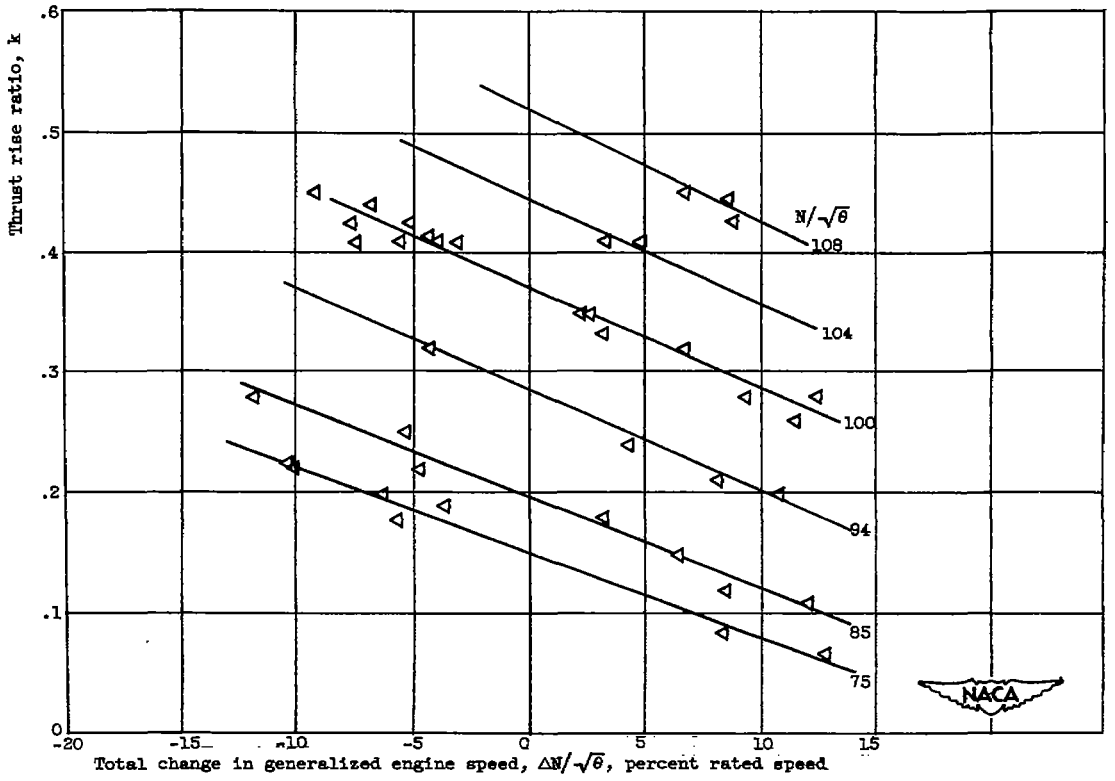

(b) Total change in generalized engine speed.

Figure 20. - Variation of thrust rise ratio with generalized engine speed and engine speed change.

[redacted]

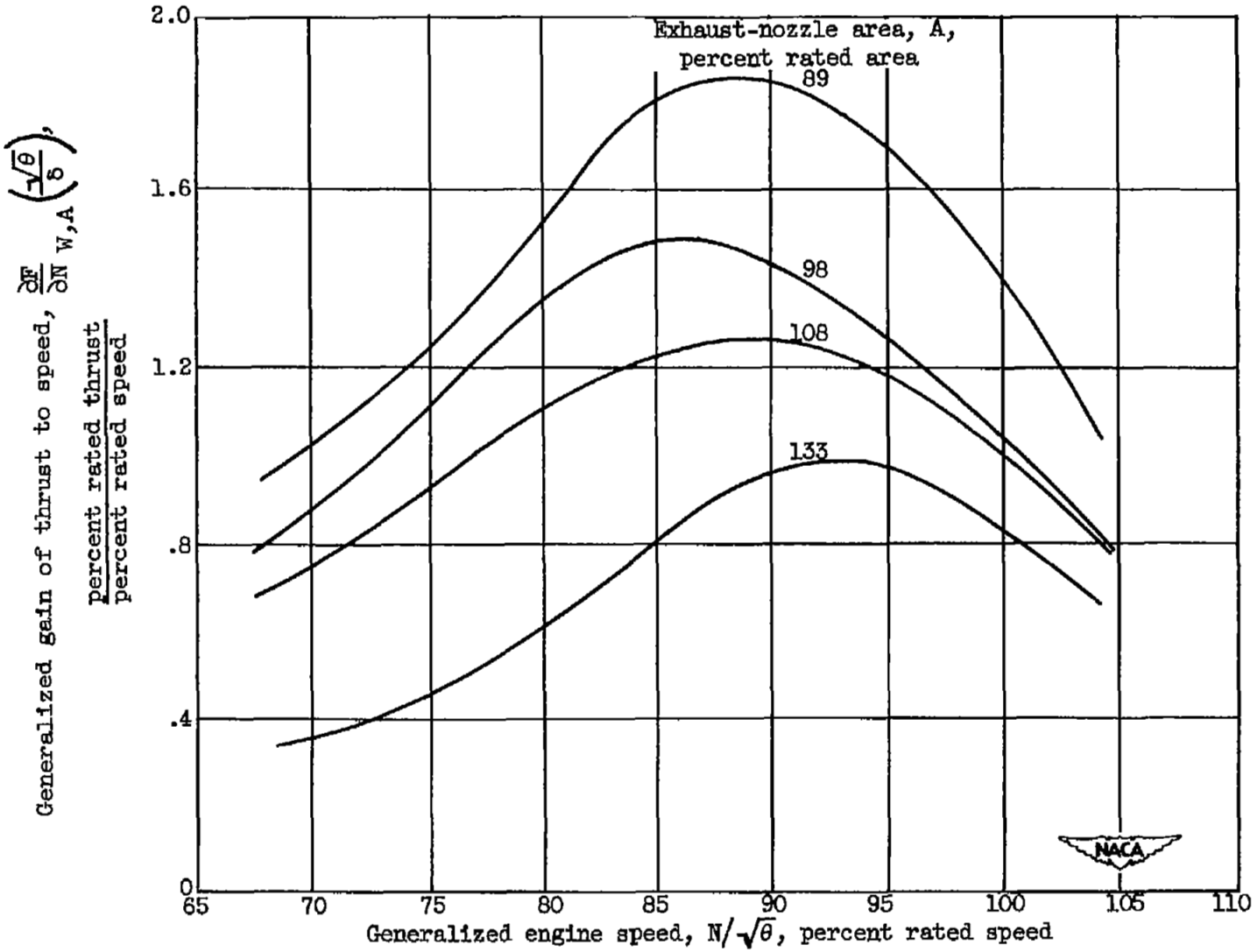

Figure 21. - Variation of generalized gain of thrust to speed with engine speed.

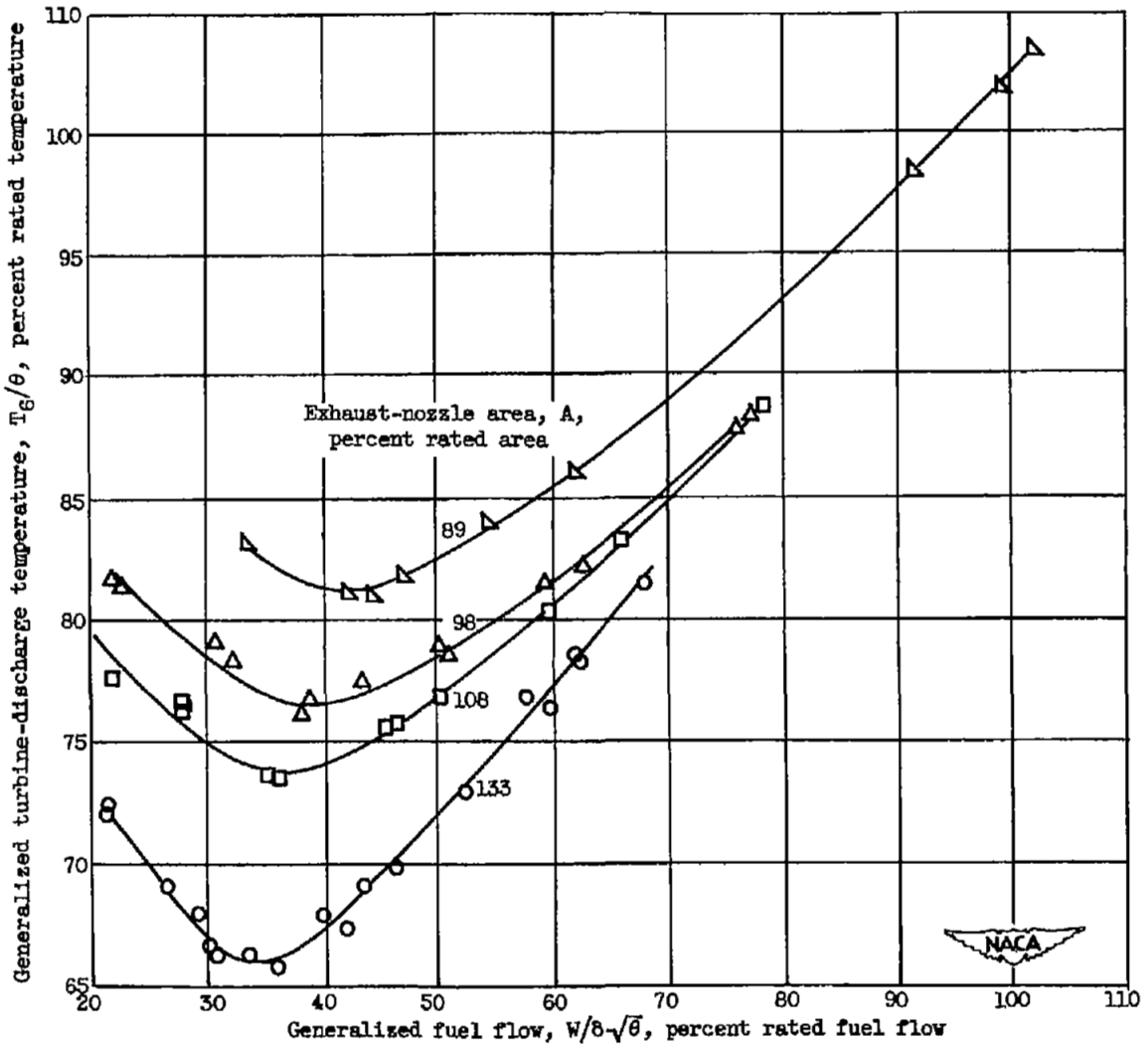

Figure 22. - Variation of generalized turbine-discharge temperature with fuel flow. Altitude, 15,000 feet; Mach number, 0.17.

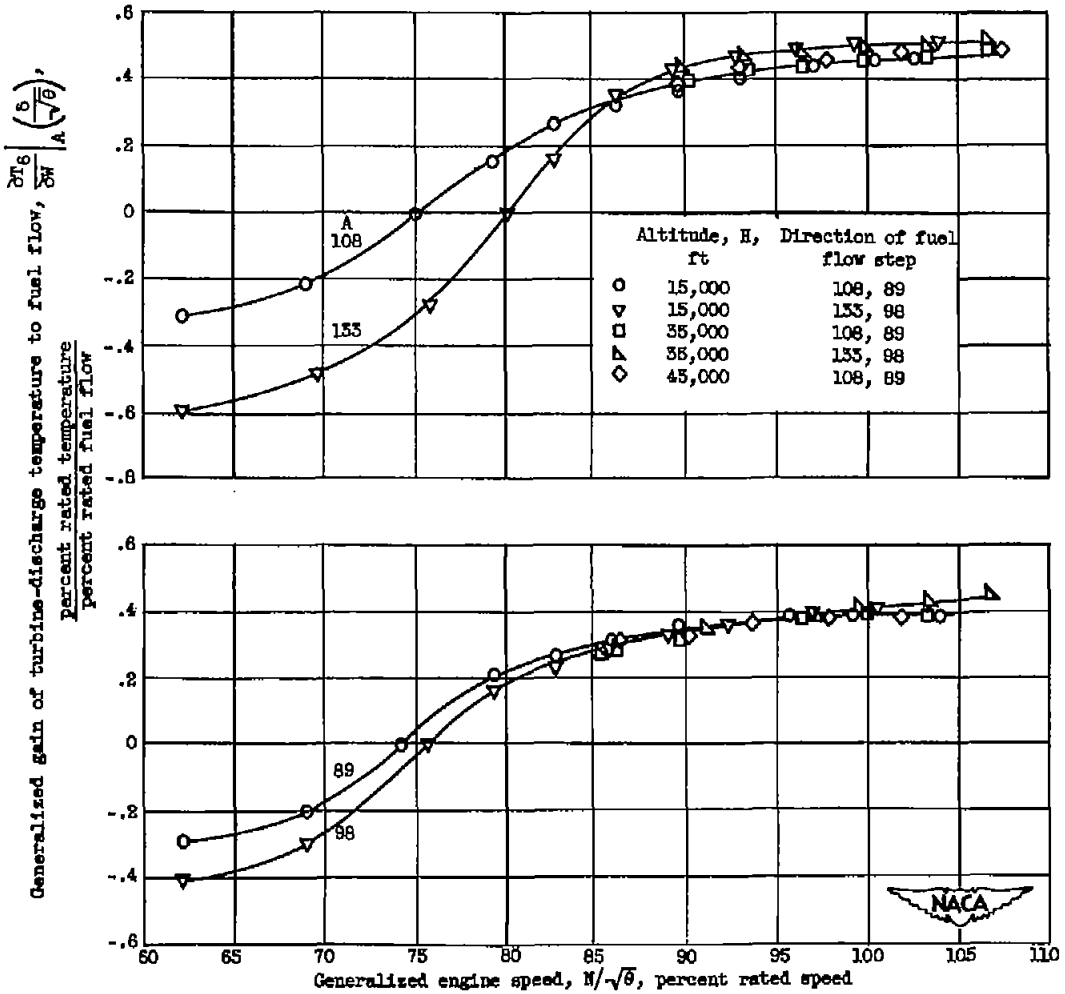

Figure 23. - Variation of generalized gain of turbine-discharge temperature to fuel flow with engine speed.

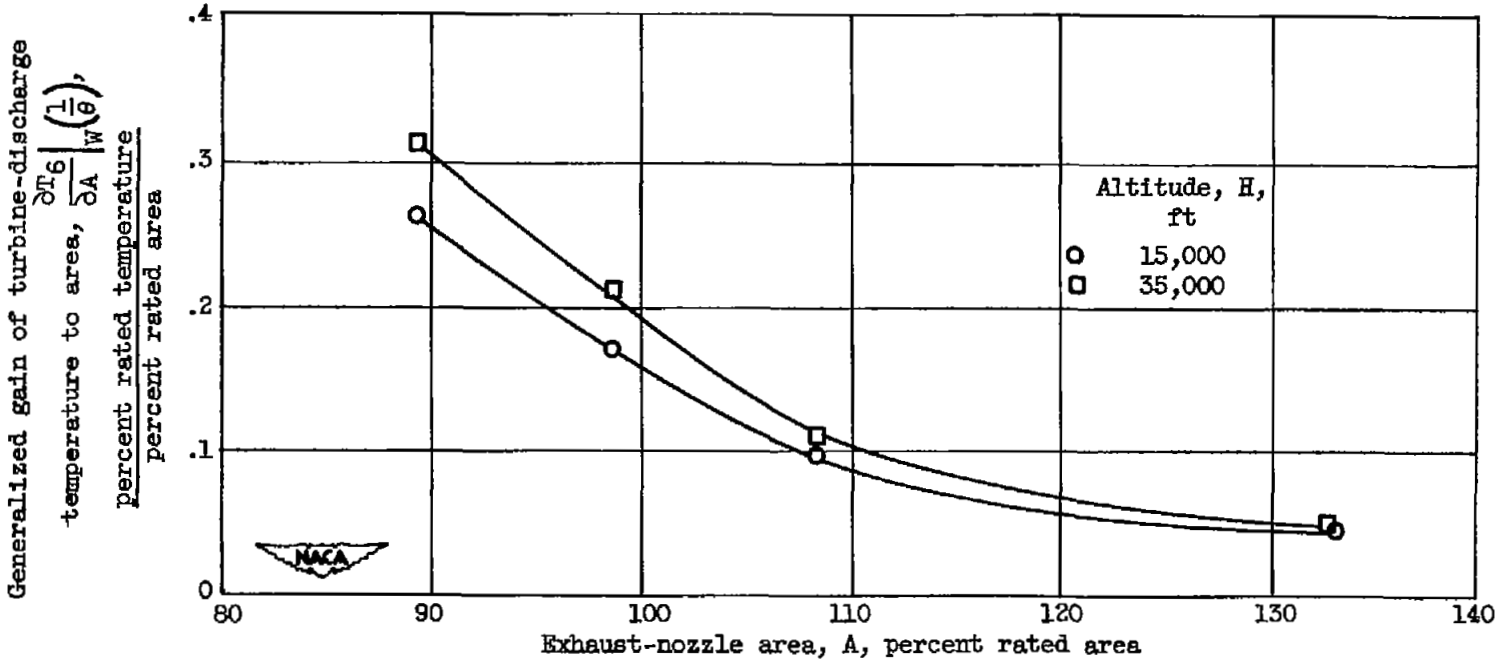

Figure 24. - Variation at 100 percent rated engine speed of generalized gain of turbine-discharge temperature to area with exhaust-nozzle area.

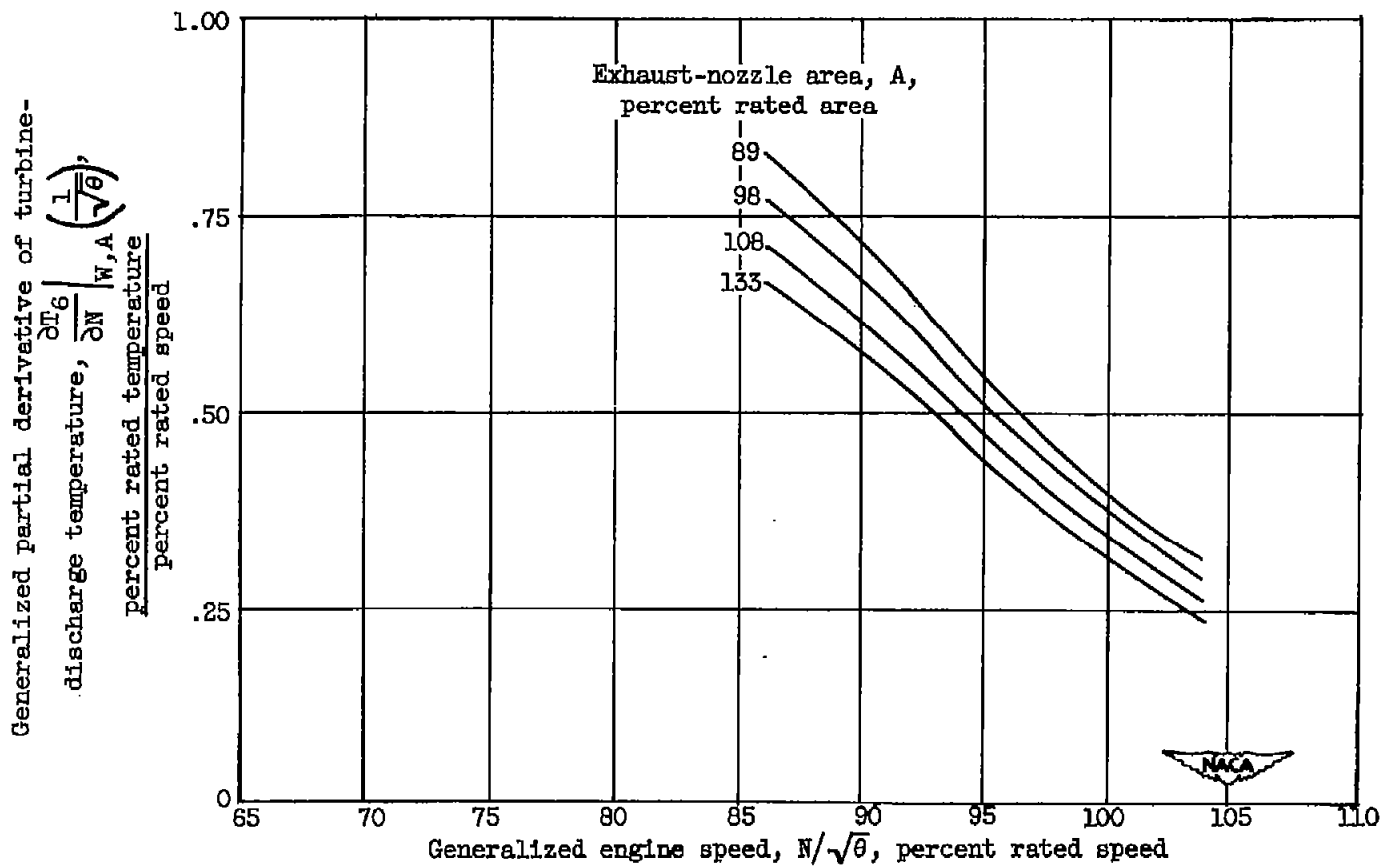

Figure 25. - Variation of generalized partial derivative of turbine-discharge temperature to speed with engine speed.

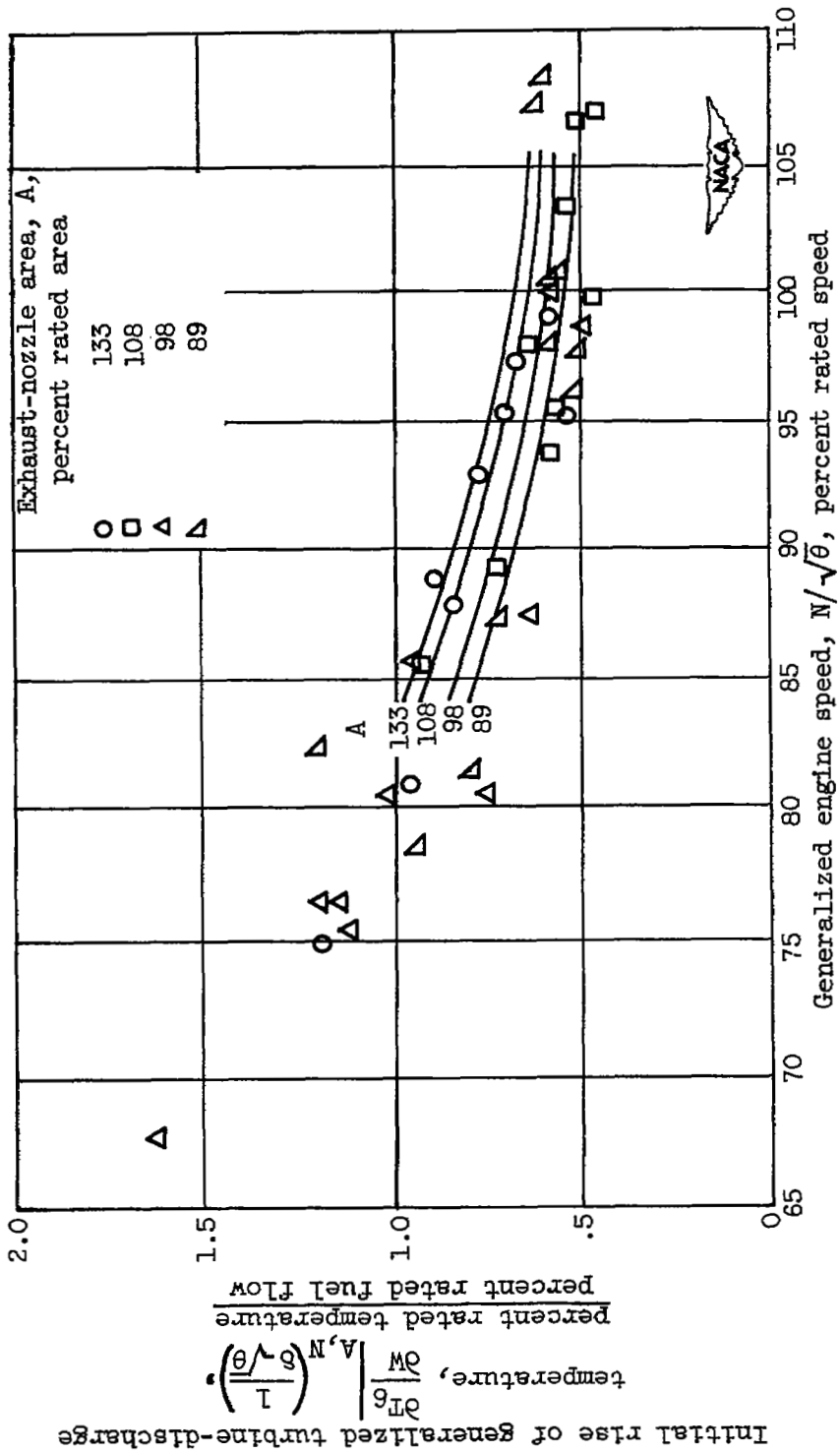

Figure 26. - Variation of initial rise of generalized turbine-discharge temperature to fuel flow step disturbances with engine speed.

[redacted]

[redacted]